UC Santa Cruz

UC Santa Cruz Previously Published Works

Title

The use of murine-derived fundic organoids in studies of gastric physiology

Permalink

https://escholarship.org/uc/item/48m5j2rj

Journal

The Journal of Physiology, 593(8)

ISSN

0022-3751

Authors

Schumacher, Michael A
Aihara, Eitaro
Feng, Rui
et al.

Publication Date

2015-04-15

DOI

10.1113/jphysiol.2014.283028

Peer reviewed

eScholarship.org Powered by the California Digital Library
University of California

The Use of Murine-Derived Fundic Organoids in Studies of Gastric Physiology

Michael A. Schumacher[1]*, Eitaro Aihara[1]*, Rui Feng[1]*, Amy Engevik[1], Noah F. Shroyer[2], Karen M. Ottemann[3], Roger T. Worrell[1], Marshall H. Montrose[1], Ramesh A. Shivdasani[4] and Yana Zavros[1]

[1] Department of Molecular and Cellular Physiology, University of Cincinnati College of Medicine, Cincinnati, OH, USA

[2] Division of Developmental Biology, Cincinnati Children's Hospital Medical Center, 3333 Burnet Avenue, Cincinnati, OH, USA

[3]Department of Microbiology and Environmental Toxicology, University of California at Santa Cruz, Santa Cruz, CA, USA

[4]Department of Medical Oncology, Dana-Farber Cancer Institute, and Department of Medicine, Harvard Medical School, Boston, MA, USA

***Authors contributed equally**

Corresponding Author:

Yana Zavros, Ph.D.

University of Cincinnati College of Medicine

Department of Molecular and Cellular Physiology

231 Albert B. Sabin Way, Room 4255 MSB

Cincinnati, OH 45267-0576

Tel: (513) 558-2421

Fax: (513) 558-5738

yana.zavros@uc.edu

key words: gastric acid secretion, gastric restitution, gastric organoids

Abbreviations: leucine-rich repeat-containing G protein-coupled receptor 5 (Lgr5), immortalized stomach mesenchymal cells (ISMCs)

Running Title: The use of fundic organoids

AUTHOR CONTRIBUTION

Michael A. Schumacher: Conception and design of the experiments, Collection, analysis and interpretation of data, Drafting the article or revising it critically for important intellectual content

Eitaro Aihara: Conception and design of the experiments, Collection, analysis and interpretation of data, Drafting the article or revising it critically for important intellectual content

Rui Feng: Conception and design of the experiments, Collection, analysis and interpretation of data, Drafting the article or revising it critically for important intellectual content

Amy Engevik: Conception and design of the experiments, Collection, analysis and interpretation of data,

Noah F. Shroyer: Conception and design of the experiments, Drafting the article or revising it critically for important intellectual content

Karen M. Ottemann: Conception and design of the experiments, Drafting the article or revising it critically for important intellectual content

Roger T. Worrell: Conception and design of the experiments, Drafting the article or revising it critically for important intellectual content

Marshall H. Montrose: Conception and design of the experiments, Drafting the article or revising it critically for important intellectual content

Ramesh A. Shivdasani*:* Conception and design of the experiments, Drafting the article or revising it critically for important intellectual content

Yana Zavros: Conception and design of the experiments, Collection, analysis and interpretation of data, Drafting the article or revising it critically for important intellectual content

ABSTRACT

Studies of gastric function and disease have been limited by the lack of extended primary cultures of the epithelium. An *in vitro* approach to study gastric development is primary mouse-derived antral epithelium cultured as 3-dimensional spheroids known as organoids. There is no report for the use of organoids for gastric function or disease. We have devised two unique gastric fundic-derived organoid cultures: *model 1)* for the expansion of gastric fundic stem cells, and *model 2)* for the maintenance of mature cell lineages. Both models were generated from single glands dissociated from whole fundic tissue and grown in basement membrane matrix (Matrigel) and organoid growth medium. Model 1 enriches for a stem cell-like niche via simple passage of the organoids. Maintained in Matrigel and growth medium, proliferating organoids expressed high levels of stem cell markers CD44 and Lgr5. Model 2 is a system of gastric organoids co-cultured with immortalized stomach mesenchymal cells (ISMCs). Organoids maintained in co-culture with ISMCs express robust numbers of surface pit, mucous neck, chief, endocrine and parietal cells. Histamine induced a significant decrease in intraluminal pH that was reversed by omeprazole in fundic organoids and indicated functional activity and regulation of parietal cells. Localized photodamage resulted in rapid cell exfoliation coincident with migration of neighboring cells to the damaged area, sustaining epithelial continuity. Thus, we report the use of these models for studies of epithelial cell biology and cell damage and repair.

INTRODUCTION

Studies of gastric function and disease have been limited to the use of *in vitro* immortalized or gastric cancer cell lines or *in vivo* animal models. An emerging *in vitro* approach that may be uniquely beneficial to study gastric physiology and disease is the primary mouse-derived epithelium cultured as 3-dimensional spheroids known as organoids. Despite the extensive use of these culture systems for the study of stem cell biology and gastrointestinal development (Barker *et al.*, 2007; Jaks *et al.*, 2008; Barker *et al.*, 2010; Stange *et al.*, 2013), the degree to which these cultures reflect the function of native tissue has not been reported. Therefore, the capacity for use in functional studies of physiological research has been limited. Our study represents a technical advance in the field of physiology. The fundic organoid culture model represents our ability to replicate the gastrointestinal environment *in vitro*, and therefore supersedes some of the existing cell line and tissue-based systems to study the mechanism of gastric acid secretion, *Helicobacter* adherence and pathogenesis, hormonal signaling and tissue repair.

The gastric epithelium is a self-renewing tissue that is anatomically divided into two major functional regions that are: 1) the fundus (or corpus) comprised of the parietal, chief, surface mucous pit and mucous neck cells, and 2) the antrum composed of predominantly mucus-producing cells. Endocrine cells are found in both the fundus and antrum (Mills & Shivdasani, 2011). Based on studies demonstrating that the leucine-rich repeat-containing G protein-coupled receptor 5 (Lgr5) may be used as a marker of stem cells in the gastric antrum, it is now possible to establish long-term primary gastric cultures (Barker *et al.*, 2007; Jaks *et al.*, 2008; Barker *et al.*, 2010).

However, such a system has not been established for the fundus (or corpus) of the stomach where Lgr5-positive cells are not expressed in the adult (Barker *et al.*, 2010). The corpus epithelium is organized into gastric units that contain the cell lineages in four distinct zones that are the surface pit, isthmus, neck and base regions (Mills & Shivdasani, 2011). Extensive studies by Karam and Leblond (Karam & Leblond, 1993) combined tritiated thymidine labeling with electron microscopy to examine the pathways of cell renewal of the gastric epithelium. Based on these studies, the isthmus region of the gastric gland is generally accepted as the zone that contains undifferentiated progenitor or 'stem' cells (Karam & Leblond, 1993). Stem cells anchored in the isthmus region are responsible for the production of parietal cells (Karam & Leblond, 1993), and distinct from the recently identified stem cells marked by *Troy* that are expressed at the corpus gland base in a subset of differentiated chief cells (Stange *et al.*, 2013). Although Stange *et al.* (Stange *et al.*, 2013) demonstrate that *Troy*-positive chief cells may be used to generate long-lived gastric organoids, *in vitro* these cultures are differentiated toward the mucus-producing cell lineages of the neck and pit regions. Our study advances these findings by not only generating an organoid culture that maintains all the major cell lineages of the fundus, but also documents the functional capacity of this system.

We have devised two unique gastric fundic-derived organoid cultures: *model 1)* for the expansion of gastric fundic stem cells that consisting of approximately 90% of CD44/Lgr5+ stem cells, and *model 2)* for the maintenance of mature cell lineages that include surface mucous pit, mucous neck, chief, endocrine, parietal and CD44/Lgr5+ cells (**Figure 1**). Model 1 enriches for a stem cell-like niche via simple passage of the

organoids. Maintained in *Matrigel* and gastric organoid growth medium, organoids were proliferative and expressed high levels of stem cell markers CD44 and Lgr5. Model 2 is a system of gastric organoids co-cultured with immortalized stomach mesenchymal cells (ISMCs) and express robust numbers of surface pit, mucous neck, chief, endocrine and parietal cells. Using these models, we demonstrate assays of epithelial barrier function, cellular restitution and pH response. The fundic organoid culture model represents a significant advance in our ability to replicate the gastrointestinal environment *in vitro*.

METHODS

Fundic organoid generation and culture

C57BL/6 or Yellow cameleon 3.0 (YC3.0) transgenic (Nyqvist *et al.*, 2005; Aihara *et al.*, 2013) mice (aged 8-10 weeks) were used for fundic and antral gastric organoid cultures. Animals were euthanized and stomachs removed, opened along the greater curvature and washed in ice-cold DPBS (Dulbecco's phosphate-buffered saline). Serosal muscle was removed from fundic or antral tissue under a dissecting microscope using micro-dissecting scissors and fine forceps (examples of preparation are shown in **Supplemental Figure 1**). There was a clear delineation and separation of collected fundic and antral tissue as shown by dotted lines in **Supplemental Figure 1**. Tissue was cut into <5 mm^2 pieces and incubated rocking at 4°C for 2 hours in Dulbecco's phosphate-buffered saline without calcium and magnesium (DPBS w/o Ca^{2+}/Mg^{2+}) +5 mM EDTA (Sigma). Tissue was removed and placed into 5 ml dissociation buffer (43.4 mM sucrose, 54.9 mM D-sorbitol (Sigma), in DPBS), and shaken vigorously for 2 minutes by hand to dissociate individual glands from tissue, followed by mechanical dissociation using a 1000 μl pipette to obtain desired gland concentration. Medium containing dissociated glands was centrifuged at 150 g for 5 minutes, and the pellet re-suspended in Matrigel (BD biosciences). Suspended glands in Matrigel were added to 12 well culture plates (50 μl Matrigel per well) or 2 well dishes (for microinjection and imaging). After Matrigel polymerization at 37°C, gastric organoid growth medium (Advanced DMEM/F12 (Life Technologies, 12634-010) containing Wnt-conditioned medium (50%), R-spondin-conditioned medium (10%), [Leu15]-Gastrin I (10 nM: Sigma), nAcetylcysteine (1mM: Sigma), FGF10 (100 ng/ml: Pepro Tech), EGF10

(Epidermal Growth Factor 10, 50 ng/ml: Pepro Tech), Noggin (100 ng/ml: Pepro Tech), and Y-27632 (initial 4 days only, 10 nM, Sigma)) was added to wells and replaced every 4 days.

To test for optimal growth and efficiency, a panel of growth conditions were assayed by removing each individual growth factor successively. Removal of EGF10, Noggin, [Leu15]-Gastrin I, Wnt-conditioned medium and R-spondin conditioned medium resulted in stunted growth and inability for organoids to survive past day 7. Use of complete medium resulted in the highest growth efficiency (**Supplemental Figure 2A, B**) and size (**Supplemental Figure 2A, C**) and demonstrated that EGF10, Noggin, [Leu15]-Gastrin I, and Wnt and R-spondin-conditioned media were necessary for growth of organoids. Interestingly removal of R-spondin conditioned medium led to a failure of organoids to grow (**Supplemental Figure 2A, B, C**). While, the removal of Wnt-conditioned medium did not inhibit the initial formation of the organoids, reduced speed of growth and failure to thrive past day 7 was observed (**Supplemental Figure 2A, B, C**).

Stem cell/progenitor expansion (model 1)

To enrich for the stem cells or progenitors, gastric organoids were passaged every 12 days. Organoids were removed from Matrigel using ice-cold DPBS, broken up by passing through a 26G needle and fractions were centrifuged at 150 g for 5 min. The pellet was re-suspended in Matrigel followed by addition of growth medium as described above.

Maintenance of epithelial cell lineages (model 2)

To maintain a mature phenotype we implemented a *Transwell* system whereby gastric organoids were co-cultured with Immortalized Stomach Mesenchymal Cells (ISMCs) (Feng *et al.*, 2014), cells previously shown to induce embryonic endoderm to differentiate to a gastric phenotype (Kim *et al.*, 2005). The ISMCs were generated by immortalizing embryonic day (E) 13.5 wild-type CD1 mouse stomach mesenchymal cell cultures with a dominant-negative Tp53-encoding retrovirus and expanding cells for multiple passages beyond the death of uninfected cells (Shaulian *et al.*, 1992). Organoids were grown in Matrigel as described above on the top side of a polyester *Transwell* insert (0.4 μm pore size, Corning) with gastric organoid medium seeded on the bottom and top of wells. At day 4, 1.2 x 10^4 ISMCs were seeded on the bottom of a 12 well plate and organoid-containing Transwell inserts were transferred to the wells. Medium and ISMCs were replaced every other day. At day 10-12 organoids were harvested for use in subsequent experiments.

Flow cytometry

Fundic gastric organoids grown with or without ISMCs were collected at day 4, 7, and 12 using ice cold DPBS. Preparation of single cells were obtained by treating organoids with dispase II (1mg/ml, Roche) for 20-30 minutes while shaking at 37^0C. Cells were labled with cell surface markers CD44 and Lgr5 using FITC rat anti-mouse CD44 (1:50, BD Pharmingen, 561859) and anti-human Lgr5 PE conjugated (1:50, OriGene, TA400001) antibodies. Cells were then fixed and permeabilized according to the manufacturer's protocol (Invitrogen Fix & Perm kit, GAS004) and then co-stained

using rabbit anti-DCAMKL1 antibody (1:33, Abcam, ab37994) followed by a 1:100 diluation of anti-rabbit IgG APC conjugated secondary antibody (Abcam, ab72567). In a separate tube of fixed and permeabilized cells, samples were incubated with lectin FITC labeled *Ulex europaeus* (UEAI, 1:100 dilution, Sigma Aldrich), lectin *Griffonia simplicifolia* Alexa Fluor 647 *(*GSII, 1:100 dilution, Molecular Probes) and then rabbit anti-intrinsic factor (1:100 dilution, Abcam, ab1322) followed by a 1:100 dilution of anti-rabbit IgG PE secondary antibody (Abcam, ab7070). In a third tube of fixed and permeabilized cells, cells were immunostained using a 1:100 dilution of anti-chromagranin A antibody (Abcam, ab15160) followed by a 1:100 dilution of anti-rabbit IgG PE conjugated secondary antibody. Finally, in a fourth tube of fixed and permeabilized cells, cells were labeled using a 1:100 dilution of anti-human gastrin (Novacastra) and anti-HK-ATPase (MA3-923, Affinity Bioreagents) antibodies followed by secondary antibodies anti-rabbit IgG APC conjugated and anti-mouse IgG FITC conjugated (Abcam, ab6785) at a 1:100 dilution. All antibody incubations were performed at room temperature for 20 minutes. Cells were analyzed using the FACSCalibur flow cytometer (BD Biosciences) and FloJo software (Tree Star, Ashland, OR).

Quantitative RT-PCR

Total RNA was isolated from gastric glands or cultured gastric organoids. cDNA was synthesized (High Capacity cDNA Reverse Transcription Kit, Applied Biosystems) and analyzed by real-time PCR (TaqMan, Applied Biosystems) using pre-validated TaqMan primers: Pepsinogen C (Mm01278038_m1), Somatostatin (Mm00436671_m1),

H^+,K^+-ATPase (Mm01176574), Gastrin (Mm00439059), Muc5AC (Mm01276711), Muc6 (Mm00725185), CD44 (Mm01277163_m1), DCLK1 (Mm00444950_m1), *Troy* (Mm00443506_m1), Cdx1 (Mm00438172_m1), Cdx2 (Mm01212280_m1), TFF2 (Mm00447491_m1), TFF3 (Mm00495590_m1), HE4 (Mm00509434_m1), MUC2 (Mm01276696_m1) and HPRT (Mm00446968_m1). PCR amplifications were performed in 20 μL containing 20X TaqMan Expression Assay primers, 2X TaqMan Universal Master Mix (TaqMan Gene Expression Systems; Applied Biosystems) and cDNA. PCR amplification (StepOne Real-Time PCR System, Applied Biosystems) used the following conditions: 50°C for 2 minutes, 95°C for 10 minutes, 95°C for 15 seconds (denature), and 60°C for 1 min (anneal/extend) for 40 cycles. LGR5 expression was quantified using specific primers for LGR5: forward- 5- CCTACTCGAAGACTTACCCAGT-3 and reverse- 5-GCATTGGGGTGAATGATAGC-3 using the SYBR Green PCR Master Mix and protocol (Applied Biosystems). Fold change was calculated as $(C_t - C_{t\,high}) = n_{target}$, $2^{ntarget}/2^{nHPRT}$ = fold change where C_t = threshold cycle. The results were expressed as average fold change in gene expression relative to the uninfected or control group, and HPRT was used as an internal control. Data were calculated according to Livak and Schmittgen (Livak & Schmittgen, 2001).

Immunofluorescence staining

Organoids were removed from Matrigel using ice-cold DPBS, and fixed in 4% paraformaldehyde for 30 minutes, followed by Histogel (Thermo Scientific) and paraffin embedding. 5μm sections were cut for immunofluorescence staining. Sections for immunofluorescence were blocked with 5% BSA before incubation with antibodies for

gastric H^+/K^+-ATPase (1:1000, Affinity Bioreagents, MA3-923) and Rhodamine-conjugated UEAI (1:5000, Vector Labs, RL-1062) overnight at 4°C. Sections were then incubated for 1 hour at room temperature with secondary antibody Alexa Fluor 633 (1:1000, Invitrogen). Sections were imaged using Zeiss LSM510.

Whole mount staining was performed on organoids 7 days of age for E-cadherin, H^+/K^+-ATPase, Intrinsic Factor, Chromogranin A. Organoids suspended in *Matrigel* were fixed with 4% paraformaldehyde for 30 minutes at room temperature, followed by tissue permeabilization with 0.5% Triton X-100 in PBS for 20 minutes, then blocking in 20% serum specific to the animal the secondary antibody was raised in. E-cadherin (1:1000, Santa Cruz, sc59778), H^+/K^+-ATPase (1:1000, Affinity Bioreagents, MA3-923), Intrinsic Factor (1:1000, Abcam, ab91322), or Chromogranin A (1:500, Abcam, ab15160) were incubated overnight at 4°C. Next, organoids were incubated with Alexa Flour 488 or 633 (1:1000, Invitrogen) for 1 hour at room temperature, followed by nuclear stain (Hoechst 33342, 10µg/ml, Invitrogen) for 20 minutes. Whole mount sections were obtained via z-stack reconstruction using the Zeiss LSM710.

EdU labeling

To identify the number of proliferating cells, gastric organoids were incubated in 5µM of 5-ethynyl-2'-deoxyuridine (EdU) (Invitrogen, C10639) in DMEM for 1 hour at 37 °C. Organoids were then fixed for 15 minutes with 3.7% formaldehyde in PBS and followed by permeabilization using 0.5% Triton X-100 in PBS for 20 minutes at room temperature. The “Click-iT” reaction cocktail (Invitrogen, C10639) was added to the cells according to the manufacturer’s instructions and incubated for 30 minutes at room

temperature, followed by 2 washes in PBS. Organoids were then incubated with DNA dye Hoechst 33342 (Invitrogen) at a dilution of 1:1000 in PBS for 30 minutes. Z-stack series of confocal images were taken using a Zeiss LSM710 LIVE Duo Confocal Microscope and analyzed using IMARIS imaging software. Total cell number and EdU-labeled nuclei were counted and expressed as EdU positive cells versus total cell ratio.

Confocal time lapse imaging microscopy

Gastric organoids were grown on chambered coverglass (Thermo Scientific) or removable Transwell inserts for live imaging. Experiments were performed with coverglass in organoid culture medium under 5% CO_2 and 37°C conditions (incubation chamber, PeCon, Erbach, Germany). The chamber was placed on an inverted confocal microscope (Zeiss LSM 710), and the growth of gastric organoid was monitored using a Zeiss EC plan-Neofluar x10 objective. Transmitted light images were collected at 30 min intervals.

Luminal pH of gastric organoid was measured using the ratiometric pH sensitive dye, 5-(and-6)-carboxy SNARF-1F or -5F (5 mM stock: EX 514 nm, EM 550-620 and 620-700 nm: Invitrogen). Dye was microinjected (23 nl) and monitored using the Plan-Apochromat x20 objective. Histamine (100 μM, Sigma) or omeprazole (100 μM, Sigma) was added to the medium. Based on changes in pH and immunofluorescence staining of the H^+,K^+-ATPase, approximately 80% of fundic organoids were classified highly responsive to treatment. Images were analyzed using MetaMorph software (Molecular Devices, Downingtown, PA). Background corrected 550-620/620-700 nm ratio values

were converted to pH using a standard curve as described previously (Chu & Montrose, 1995).

Transmission electron microscopy

Organoids were fixed in 2% glutaraldehyde plus 2% paraformaldehyde in 0.1M sodium cacodylate buffer (pH 7.4) overnight at 4^{o}C. Organoids were then washed using 0.1M sodium cacodylate buffer followed by a 1 hour incubation using 4% osmium tetroxide, washed and then dehydrated using 25-100% ethanol (series of dilutions), embedded using propylene oxide/LX112. Blocks were sectioned (150 nm) and stained with 2% uranyl acetate followed by lead citrate. Tissue was visualized using a Hitachi transmission electron microscope equipped with an AMT Image Capture Engine version 5.42.366 and MicroFIRE by Optronics camera.

Acridine Orange experiments

Organoids were incubated with Acridine Orange (1 μM) for 15 min at 37°C/5% CO_2. Fluorescence of acridine orange was excited at 458 nm or 488 nm and images were collected in a time series at 600-650 nm or 500-550 nm, respectively. At each time point, a set of ten XY-plane images were taken at 6 μm focus intervals. Histamine (final concentration of 100 μM) was applied to the medium.

Images were analyzed by MetaMorph software (ver.6.3, Molecular Devices). The background-corrected F458/F488 fluorescence ratio image was calculated and normalized to a value of 1 in the histamine pretreatment baseline. The 3D images were created by Imaris software (ver.7.7 Bitplane).

Induction of laser-induced microlesion

Organoids in the PeCon chamber (5% CO_2, 37^0C) were placed on the stage of an inverted confocal/two-photon microscope (Zeiss LSM 510 NLO) and imaged with a C-Achroplan NIR X40 objective. The organoid was pre-incubated with nuclear stain, Hoechst (10 μg/ml: Invitrogen), for 30 min while Lucifer yellow (50 μM: Invitrogen) was applied before the experiment. Confocal imaging recorded organoid structure (confocal reflectance 730 nm), Hoechst (EX: 730 nm, EM 435-485 nm), YFP (EX: 514 nm, EM: 535-585 nm) or Lucifer yellow (EX: 458 nm, EM 500-550 nm). The method of causing microscopic photodamage in the tissue with a two-photon laser has been described previously (Xue *et al.*, 2011). Briefly, after collecting a set of control images using minimal Ti-Sa (730nm) laser power (< 50 mW), a small rectangular region (< 10 μm^2) of cells was repetitively scanned (700-1000 mW average laser power), for 150 iterations.

Statistical Analyses

The significance of the results was tested by Student's t-test using commercially available software (GraphPad Prism; GraphPad Software, San Diego, CA). $P < 0.05$ was considered significant.

RESULTS

Fundic gastric organoids enriched for stem cells

Figure 2 demonstrates our ability to maintain a long-term culture system for the fundic region of the mouse stomach. Fundic and antral gastric glands formed cyst-like structures visible within 3 days of culture (**Figure 2A**). We determined the gene expression of gastric-specific cell lineage markers prior to the first passage. Both fundic and antral organoids, expressed mRNA for mucin 5AC (surface mucous pit cells), mucin 6 (mucous neck cells), pepsinogen C (zymogen/chief cells) and somatostatin (D cells) as detected by qRT-PCR (**Figure 2B**). In contrast, the expression of gastrin (G cells) was specific to antral organoids, whereas H^+,K^+-ATPase (parietal cells) was specific to fundic organoids (**Figure 2B**). Time-lapse imaging of organoid formation over the initial 72 hours showed proliferating cells of fundic gastric glands localized to a mid-gland region (**Supplemental Video 1**) as opposed to the base on antral glands (**Supplemental Video 2**). Subsequently, proliferative regions of both antral and fundic glands expanded into epithelial spheroids.

Epithelial polarity was confirmed by apical membrane staining of *Ulex Europaeus* I (UEAI) lectin on surface mucous pit cells (**Figure 2C**) and basolateral membrane staining for E-cadherin (**Figure 2C**). Moreover, luminal retention of micro-injected Lucifer yellow over 24 hours confirmed the low transepithelial permeability of fundic organoids (**Supplemental Fig. 3B-E**).

Prior to the first passage of the organoids, we confirmed cell-specific expression of parietal, chief and endocrine cell markers by immunostaining (**Figure 2D**). To quantify the cellular composition we performed flow cytometric analysis of major gastric

cell lineages using fundic organoids cultured for 4, 7 and 12 days. With culture the percentage of parietal, endocrine, chief, and surface pit cells declined, however, a population of cells co-expressing stem cell markers CD44 (Khurana *et al.*, 2013) and Lgr5 (Barker *et al.*, 2010) were enriched (**Figure 2E, F**). These data were confirmed by qRT-PCR demonstrating a decrease in cell lineage markers (**Figure 2G**) that correlated with an increase in stem cell markers (**Figure 2H**). While cells expressing stem cell markers CD44 and Lgr5 expanded with passaging, *Troy* expression declined (**Figure 2G**). We have cultured fundic gastric organoids for over 90 days (**Supplemental Figure 3A**). Therefore, our ability to sustain the fundic organoids in culture for several passages with an expansion in a cellular composition of cells expressing stem cell markers CD44 and Lgr5 suggests enrichment for a stem cell-like niche.

Maintenance of mature cell lineages within fundic gastric organoids

We next sought to develop a protocol to maintain the differentiated phenotype within the fundic gastric organoids. We adopted an approach used by investigators to drive embryonic gastric epithelial differentiation (Kim *et al.*, 2005; Kim *et al.*, 2011) using mouse-derived immortalized stomach mesenchymal cells (ISMCs) in co-culture (**Figure 3A**). By 3 days in co-culture the organoids displayed glandular structures and budding of the epithelium (**Figure 3A**). Immunofluorescence staining of the H^+,K^+-ATPase-expressing parietal cells were elevated in organoids co-cultured with ISMCs (**Figure 3B**) that were then quantified using flow cytometry. Flow cytometric analysis revealed that co-culture induced or maintained expression of major cell lineages (**Figure 3C**, **Supplemental Figure 3F-K**). In addition, there were significantly lower numbers of

CD44/Lgr5-positive cells associated with model 2 in comparison to model 1 that may be a reflection of decreased stem cell proliferation in a system of sustained mature epithelial cells (**Figure 3D**). We concluded that with ISMC co-culture an epithelium expressing mature tissue markers is maintained.

To determine the proliferative capacity of the cells within models 1 and 2, cultures were immunostained for EdU and proliferating cells quantified (**Figure 3E, F**). While there was maintenance of proliferating cells in the co-culture model 2 system, there was a significant decrease in the number of proliferating cells in model 1 (**Figure 3E, F**). Proliferation was restored in model 1 after passage (data not shown). Cells within the model 1 culture system increased in proliferation after passage (data not shown). Such data suggests that the gastric organoids in model 1 cannot be maintained in culture indefinitely without passage.

Markers of intestinal metaplasia and SPEM are expressed in cultured fundic gastric organoids

We observed that the one differentiated marker that increased in model 1 was GSII (**Figure 2E**). Given that this marker has also been implicated in the development of metaplasia, in particular spasmolytic polypeptide expressing metaplasia (SPEM) (Nozaki K, 2008), other metaplastic markers were measured by qRT-PCR in models 1 and 2 at 4, 7 and 12 day cultures (**Figure 4**). When compared to the expression levels in native tissue, expression of markers of intestinal metaplasia that included Cdx1 (**Figure 4A**), MUC2 (**Figure 4C**) and TFF3 (**Figure 4D**) significantly decreased in both models with culture. However compared to the native tissue, Cdx2 expression was

significantly upregulated in models 1 and 2 day 4 cultures (**Figure 4B**). Expression of Cdx2 significantly decreased in both models over 12 days in culture (**Figure 4B**). HE4, typically elevated during metaplasia (Nozaki K, 2008), significantly increased in the organoid cultures relative to expression in the native tissue (**Figure 4E**). While TFF2 was significantly increased in model 1 over 12 days in culture, expression of TFF2 significantly decreased in model 2 over time (**Figure 4F**). Collectively, these data show that Cdx2, a marker of intestinal metaplasia (Moskaluk *et al.*, 2003), was upregulated during the initial culture of the gastric organoids. In addition, SPEM marker HE4 was also increased in the gastric organoids compared to expression levels in native tissue.

Fundic gastric organoids are comprised of functional parietal cells

To assess parietal cell function, a pH-sensitive dye was injected into the lumen of organoids with or without ISMC co-culture. Histamine induced a significant decrease in intraluminal pH that was reversed by omeprazole in fundic organoids (**Figure 5A, B**). Notably the response to histamine and omeprazole was greater in co-cultured organoids (**Figure 5B**). Antral-derived cultures appeared to respond to histamine but not to omeprazole treatment (**Figure 5C, D**). The changes in pH observed in the antral-derived organoids may be attributed to metabolic changes. Moreover, the lack in response to omeprazole within the antral-derived cultures suggests that the response to histamine was not attributed to parietal cell function. Thus, fundic gastric organoids were also found to maintain a functional epithelium. These data demonstrate a primary culture system of healthy fundic gastric organoids that retain differentiated epithelial characteristics.

Transmission electron microscopy revealed a secretory membrane in parietal cells within the organoids. The parietal cells within the organoids exhibited well-developed canaliculi that appeared to be well organized within the cell with long microvilli (**Figure 6A, B**). Therefore, we further investigated whether the parietal cells in the fundic organoids are capable of acid secretion in response to histamine. Acridine Orange, a fluorescence dye, is known to show green fluorescence (Maximum Ex: 503 nm Em: 526 nm) at a neutral pH, whereas its fluorescent spectrum shifts to red (Maximum Ex: 460 nm, Em: 650 nm) when it accumulates in the acidic organelles, such as the secretory canaliculus of parietal cell (Lambrecht *et al.*, 2005). In response to histamine, Acridine Orange accumulated in cell vesicles as indicated in **Figure 6C** (cells identified by white circles 1-5), which was accompanied by an increase in the ratio of F458(red)/F488 (green) (**Figure 6D**). These results indicated the generation of protons present within the secretory canaliculi. No accumulation was observed before histamine treatment. Collectively, these results indicate that functional parietal cells exist in the fundic organoids.

Fundic gastric organoids used to study epithelial restitution

We used an established photodamage model of cell damage (Xue *et al.*, 2011; Aihara *et al.*, 2013) to test the use of fundic organoid culture in studies of cell migration/repair. Localized photodamage (**Figure 7A, red rectangle**) resulted in the loss of YFP and rapid dead cell exfoliation (**Figure 7A, arrow 2**) coincident with migration of neighboring cells to the damaged area (**Figure 7A, arrow 3**), sustaining epithelial continuity (**Figure 7A, arrow 4**), similar to what is seen *in vivo* (Nyqvist *et al.*,

2005; Xue *et al.*, 2011; Aihara *et al.*, 2013) (**Supplemental Video 3**). Damaged cells were exfoliated into the lumen following photodamage, while lucifer yellow did not leak into the lumen, suggesting that the integrity of the epithelium was maintained (**Figure 7B**).

DISCUSSION

The fundic organoid culture model represents a significant advance in our ability to replicate the gastrointestinal environment *in vitro*. We concluded from these studies that: 1) with extended culture, fundic gastric organoids are an ideal model for the enrichment of a stem cell-like niche, 2) with ISMC co-culture an epithelium expressing mature cell lineages can be maintained *in vitro*, and 3) fundic gastric organoids can be used for the study of gastric physiology and disease (**Figure 1**). Major efforts were made to produce the gastric organoids specifically from the fundic region of the stomach because of the advantages this model has over existing models. For example, the simple AGS gastric cancer cell line is a useful tool for studying *Helicobacter pylori* (*H. pylori*) adherence and pathogenesis (Zhang *et al.*, 2002). However, despite extensive evidence demonstrating that *H. pylori* induces gastric epithelial changes, the direct impact of the bacterium on the normal gastric epithelium independent of systemic factors has never been studied. The gastric organoids make it possible for us to study the direct interaction between the bacteria and the normal gastric epithelium (Schumacher *et al.*, 2014). Furthermore, gastric acid secretion can be measured in isolated gastric glands (Lambrecht *et al.*, 2005), but unlike the organoid culture system, gastric glands cannot be maintained indefinitely *in vitro* making long term studies difficult. Thus, overall cultured stem cells into gastric organoids certainly have advantages over these simpler *in vitro* systems.

Cellular quantification for the major gastric cell lineage markers demonstrated that with extended culture we enriched for a stem cell-like niche. By day 12 and following passage of organoids, there was a decrease in the relative expression of

mature cells within the organoid. However, reported markers for putative gastric stem cells such as Lgr5 (Barker *et al.*, 2010) and CD44 (Khurana *et al.*, 2013) were increased. The hyaluronic receptor CD44 (Aruffo *et al.*, 1990) has been identified as a potential gastric stem cell marker of the fundus. Notably, CD44-positive undifferentiated cells have been located within the isthmus region of the fundus, precisely where the stem cells are known to reside (Khurana *et al.*, 2013). Unpublished data from our laboratory also show that single CD44-positive cells isolated from the fundus give rise to organoids in culture. Thus CD44-positive cells have the capacity to undergo cell division that may give rise to differentiated gastric epithelial cells. The increase in Lgr5 was surprising given that this stem cell marker is expressed in the fundus during development alone (Barker *et al.*, 2010), and suggests a reversion from a mature to an immature phenotype when using the specified gastric organoid growth culture conditions.

While cells expressing stem cell markers CD44 and Lgr5 expanded with passage, *Troy* expression declined. It is accepted that stem cells anchored in the isthmus region are responsible for the production of parietal cells (Karam & Leblond, 1993), and appear to be distinct from the recently identified stem cells marked by *Troy* (Stange *et al.*, 2013). *Troy*-positive cells are expressed at the corpus gland base in a subset of differentiated chief cells (Stange *et al.*, 2013). Stange *et al.* (Stange *et al.*, 2013) demonstrate that *Troy*-positive chief cells may be used to generate long-lived gastric organoids, and *in vitro* these cultures are differentiated toward the mucus-producing cell lineages of the neck and pit regions. The *Troy*-derived organoids are distinct from the cultures that are derived from whole dissociated glands reported here

such that we have devised a method to maintain all the major cell lineages of the fundus.

To maintain a mature phenotype we implemented a Transwell system whereby gastric organoids were co-cultured with Immortalized Stomach Mesenchymal Cells (ISMCs) (Shaulian *et al.*, 1992). We observed a significant induction in the expression of the major cell lineages when compared to the expression levels of 12 day-old organoid cultures. The ISMCs are shown to induce embryonic endoderm to differentiate to a gastric phenotype (Kim *et al.*, 2005). An interesting study by Kim *et al*. (Kim *et al.*, 2005) demonstrated that by epithelial-mesenchymal co-cultures homeobox gene Barx1 (normally confined to the stomach mesenchyme) drives stomach epithelial differentiation via the inhibition of Wnt signaling. Therefore, we may speculate that in the current co-culture system Barx1 may play a similar role in the differentiation of the gastric organoids, but this requires further investigation.

Cdx2, a marker of intestinal metaplasia (Moskaluk *et al.*, 2003), was upregulated during the initial culture of the gastric organoids. These data suggest that initially the cultures are metaplastic and with type in culture cells revert back to normal differentiation. SPEM marker HE4 was also increased in the gastric organoids when compared to expression levels in native tissue. HE4 has been shown to be up-regulated in gastric metaplasia in both mice and humans and its expression is maintained in gastric adenocarcinomas (Nozaki K, 2008). Although HE4 was upregulated initially in the gastric organoids, expression significantly decreased with culture time in model 2. Interestingly, it has been suggested that SPEM cells re-differentiate to chief cells in the process of tissue repair such as that observed during ulcer healing (Kikuchi *et al.*,

2010). Perhaps HE4 is up-regulated in the organoids as a mechanism of cellular proliferation and repair during the development of the spheres. Notably, TFF2 significantly increased over time in model 1. Consistent with the enrichment of stem cells in model 1 of our gastric organoids cultures, TFF2 transcript-expressing cells have been shown to be progenitors for mucus neck, parietal and zymogenic cells in the oxyntic gastric mucosa (Quante *et al.*, 2010).

Fundic gastric organoids were also found to maintain a functional epithelium. Histamine induced a significant decrease in intraluminal pH that was reversed by omeprazole in fundic organoids. These observations supported numerous physiological studies showing that histamine released from the enterochromaffin-like (ECL) cells stimulates acid secretion from parietal cells within the gastric epithelium (Prinz *et al.*, 1993; Waldum *et al.*, 1996). Omeprazole blocks histamine-induced acid secretion by specifically binding to the H^+,K^+-ATPase on the parietal cells (Wallmark *et al.*, 1983). Notably the response to histamine was greater in co-cultured organoids and correlated with the presence of greater numbers of parietal cells within the epithelium. In contrast to the fundic organoids, while antral-derived cultures respond to histamine these cultures do not respond to omeprazole. The changes in pH observed in the antral-derived organoids may be attributed to metabolic changes. The lack in response to omeprazole within the antral-derived cultures suggests that the response to histamine was not attributed to parietal cell function. Overall, there was a minor pH difference with surrounding media compared to the *in vivo* pH of the stomach. This high pH in vitro is attributed to the buffering of the surrounding media and also the significantly lower number of parietal cells within organoids compared to native tissue. In addition, we

demonstrated that the fundic organoid culture may be used in studies of cell migration/repair. Localized photodamage consistently resulted in rapid dead cell exfoliation into the lumen similar to what is seen *in vivo* (Nyqvist *et al.*, 2005; Xue *et al.*, 2011; Aihara *et al.*, 2013). Moreover, neighboring cells formed lamellipodia and migrated toward and sealed the damaged area, suggesting that gastric organoids may also be used for the study of cell migration. These data demonstrate a primary culture system of healthy fundic gastric organoids that retain differentiated epithelial characteristics and mimic the native tissue responses.

Although the organoid culture system has been extensively used for the study of stem cell biology and gastrointestinal development (Barker *et al.*, 2007; Jaks *et al.*, 2008; Barker *et al.*, 2010; Stange *et al.*, 2013), here we report for the first time the degree to which these cultures reflect the function of native tissue. Moreover, we detail the cellular nature of two fundic gastric organoids culture models and the capacity for use in functional studies of physiological research. We have developed two gastric fundic-derived organoid spheroid cultures. Model 1 can be used for the expansion of gastric fundic stem cells for studies that may include stem cell biology and tissue repair/regeneration (**Figure 1**). Model 2 can be used for studies of physiological function gastric disease and epithelial cell biology whereby the maintenance of mature cell lineages is required (**Figure 1**). These results suggest that gastric fundic organoids have utility in studies of epithelial cell biology, cell damage and bacterial-epithelial interactions.

In the past, the small intestinal submucosa was used as a scaffold for gastrointestinal restoration because of its acellular biodegradable collagen-rich matrix

containing functional growth factors, such as basic fibroblast growth factor (bFGF), vascular endothelial growth factor (VEGF) and transforming growth factor-β (TGFβ), which are considered vital to the regenerative process (Voytik-Harbin *et al.*, 1997; McDevitt *et al.*, 2003; Hodde *et al.*, 2007). The small intestinal submucosa has been commonly used as a bioscaffold for the replacement of various gastrointestinal tracts in animals, including the esophagus (Doede *et al.*, 2009), small intestine (Chen & Badylak, 2001; Wang *et al.*, 2003; Lee *et al.*, 2008; Qin & Dunn, 2011), colon (Ueno *et al.*, 2007b; Hoeppner *et al.*, 2009) and stomach (de la Fuente *et al.*, 2003; Ueno *et al.*, 2007a; Nishimura *et al.*, 2010; Nakatsu *et al.*, 2013). Alternatively, adult stem cell therapy using gastrointestinal organoids may hold promise for the treatment of gastrointestinal diseases. The feasibility of colon stem cell therapy based on the simple *in vitro* expansion of a single adult colonic stem cell has been reported (Yui *et al.*, 2012). However, whether gastric-derived organoids may be used for stomach regeneration and the treatment of disease remains to be investigated.

FIGURE LEGENDS

Figure 1: Schematic diagram showing the development of 2 organoid culture systems that may be used for studies of gastric physiological function and disease. *Model 1* represents a system whereby stem/progenitor cells are expanded for studies in stem cell biology and tissue repair/regeneration. *Model 2* represents a culture system of maintained epithelial cells for studies of physiological function, gastric disease and epithelial cell biology.

Figure 2: Model 1: Fundic gastric organoids used in the expansion of stem/progenitor cells. (**A**) Cyst-like 3-D structures grown from fundic or antral gastric glands isolated from mouse. Images from 0, 3, 7 and 12 day cultures. Scale bars = 50μm. (**B**) RT-PCR analysis of gastric lineage markers at culture day 12. Both fundic and antral organoids expressed mRNA for mucin 5AC (surface mucous pit cells), mucin 6 (mucous neck cells), pepsinogen C (zymogen/chief cells), and somatostatin (D cells). In contrast, the expression of gastrin (G cells) was specific to antral organoids whereas H^+,K^+-ATPase (parietal cells) was specific to fundic organoids. (**C**) Organoid sections immunostained for H^+,K^+-ATPase (HK, green) and UEAI (red), and E-cadherin (red) and Hoechst (nuclear, blue) Scale bars = 20μm. (**D**) Organoids immunostained for HK (red), chromogranin A (chgA, red), intrinsic factor (IF, red), and, Hoechst (nuclear, blue). Scale bars = 50μm. (**E**) Flow cytometric analysis using fundic organoids 4, 7 and 12 days in culture. (**F**) 2D flow cytometric histogram of gated cells co-expressing CD44 and

Lgr5. (**G, H**) qRT-PCR of cell lineage and gastric stem cell markers using RNA isolated from organoids cultured for 3, 7 and 12 days. * P<0.05 compared to day 4,
n = 4 individual organoids preparations.

Figure 3: Model 2: Maintenance of epithelial cells within fundic gastric organoids co-cultured with ISMCs. (**A**) Organoid/ISMC co-culture *Transwell* system showing morphological changes in organoids. (**B**) Organoids in whole mount immunostained for H^+,K^+-ATPase (HK, red), and Hoechst (nuclear, blue) co-cultured without (W/O) or with (W/) ISMCs. (**C**) Flow cytometric analysis using fundic organoids co-cultured with ISMCs for 4, 7 and 12 days in culture. (**D**) 2D flow cytometric histogram of gated cells co-expressing CD44 and Lgr5. (**E**) EdU immunostaining (EdU:red, nuclear:blue) followed by (**F**) quantification of Edu+ nuclei/total cell number.

Figure 4: Expression of metaplastic markers in cultures of gastric organoids of model 1 and model 2. Quantitative RT-PCR of metaplastic markers (**A**) Cdx1, (**B**) Cdx2, (**C**) MUC2, (**D**) TFF3, (**E**) HE4 and (**F**) TFF2 using RNA isolated from organoids cultured for 4, 7 and 12 days. * P<0.05 significantly decreased compared to native tissue, # P<0.05 significantly increased compared to native tissue, n = 3 individual organoid preparations.

Figure 5: Organoid-derived parietal cell functional assay. Intraluminal pH response to histamine (His) and omeprazole (Ome) using fundic organoids cultured (**A**) without (W/O) ISMCs or (**B**) with (W/) ISMCs. Intraluminal pH response to His and Ome

using antral organoids cultured (**C**) W/O ISMCs or (**D**) W/ ISMCs. n = 6 individual organoids.

Figure 6: Presence of parietal cells in the fundic gastric organoids. Observation of parietal cells within the fundic organoid in low (**A**) or high (**B**) magnification by transmission electron microscopy. N: Nuclear, M: Mitochondria. (**C**) Confocal images of fundic organoid labeled with Acridine Orange before and after histamine (100 µM). Images shows 3D, 2D or pseudocolor of F458 (Red)/F488 (Green), respectively. (**D**) Changes of the ratio F458/F488 in response to histamine from 5 individual cells indicated in **C**.

Figure 7: Fundic gastric organoids used to study epithelial restitution. (**A**) 2-photon damage (at site indicated by arrow 1 and red box) results in cell exfoliation into the lumen and restoration of the damaged epithelium within 30 min. Blue=nuclear stain; Green=endogenous YFP cytoplasmic fluorescence of fundic organoids from YC transgenic mouse cells. (**B**) Maintenance of epithelial barrier following cell damage. 2-photon damage (at site indicated by arrow 1 and red box) results in cell exfoliation into the lumen and restoration of the damaged epithelium within 30 min. The entrance of Lucifer yellow-containing extraluminal medium into the lumen of the organoid is limited. Blue = nuclear stain; Green = Lucifer yellow; Red = Reflectance.

Supplemental Video 1: Growth of fundic-derived organoid.

Supplemental Video 2: Growth of antral-derived organoid.

Supplemental Video 3: 2-photon induced damage (photodamage, PD) at fundic organoid apical side repairs rapidly with cell exfoliation to lumen. Red = reflectance, Blue = nuclei, Green = YFP, and merged. PD created at 30 sec at cell indicated by arrow.

Supplemental Figure 1: Fundic and antral dissection. Stomachs were opened along the greater curvature, and washed in ice-cold DPBS. Stomachs were pinned and muscle was stripped using dissecting scissors and microscope. Images before and after muscle stripping are shown for fundus and antrum. Tissue collected for gland isolation is shown in dotted lines demonstrating collection of distinct regions for fundus and antrum for organoid preparation.

Supplemental Figure 2: Determination of optimal growth conditions for fundic gastric organoids. (**A**) The requirement for growth factors is demonstrated in representative images at day 7 of culture. (**B**) Fundic organoid growth efficiency (% organoids per glands seeded) and (**C**) size (at day 7) was assayed in primary cultures by removing each individual growth factor from growth medium.

Supplemental Figure 3: (**A**): Fundic gastric organoid maintained in culture for 90 days. (**B-E**) Injection and retention of Lucifer yellow (LY) within the organoid lumen after injection. Luminal retention of microinjected Lucifer yellow over 24 hours confirmed low

transepithelial permeability of fundic organoids. Stereoscope images of organoids during LY injection in brightfield (**B**) or fluorescence (**C**). Confocal image of organoids 1 day after LY injection in brightfield (**D**) or fluorescence plus brightfield (**E**). (**F-K**) Representative flow cytometric dot plots showing the gating scheme and cell distribution of UEAI (surface pit), GSII (mucous neck), IF (intrinsic factor, chief), ChgA (endocrine), and HK (H, K-ATPase, parietal) cells in gastric organoids.

ACKNOWLEDGEMENTS

This work was supported by the American Gastroenterological Association: Robert and Sally Funderburg Research Award in Gastric Cancer and R01 DK083402 grant (Zavros), the Albert J. Ryan Fellowship (Schumacher) and R01 DK54940 (Montrose). This project was supported in part by PHS Grant P30 DK078392 (Integrative Morphology Core) and NIH AR-47363 (Research Flow Cytometry Core in the Division of Rheumatology) of the Digestive Diseases Research Core Center in Cincinnati. We gratefully acknowledge Drs. Meritxell Huch, Sina Bartfeld, and Hans Clevers (Hubrecht Institute for Developmental Biology and Stem Cell Research, Netherlands) for the kind gift of L-cell and the technical discussion. We also acknowledge Dr. Jeffrey Whitsett for kindly donating the modified HEK-293T cells (Section of Neonatology, Perinatal and Pulmonary Biology, Cincinnati Children's Hospital Medical Center and The University of Cincinnati College of Medicine, Cincinnati, OH). We thank Lisa MacMillan (Pathology Research Core, Cincinnati Children’s Hospital Medical Center) for embedding and tissue processing.

REFERENCES

Aihara E, Hentz CL, Korman AM, Perry NP, Prasad V, Shull GE & Montrose MH. (2013). In vivo epithelial wound repair requires mobilization of endogenous intracellular and extracellular calcium. *J Biol Chem* **288,** 33585-33597.

Aruffo A, I. S, Melnick M, Underhill CB & Seed B. (1990). CD44 is the principal cell surface receptor for hyaluronate. *Cell* **61,** 1303-1313.

Barker N, Huch M, Kujala P, van de Wetering M, Snippert HJ, van Es JH, Sato T, Stange DE, Begthel H, van den Born M, Danenberg E, van den Brink S, Korving J, Abo A, Peters PJ, Wright N, Poulsom R & Clevers H. (2010). Lgr5(+ve) stem cells drive self-renewal in the stomach and build long-lived gastric units in vitro. *Cell Stem Cell* **6,** 25-36.

Barker N, van Es JH, Kuipers J, Kujala P, van den Born M, Cozijnsen M, Haegebarth A, Korving J, H. B, Peters PJ & Clevers H. (2007). Identification of stem cells in small intestine and colon by marker gene Lgr5. *Nature* **449,** 1003-1007.

Bell SM, Schreiner CM, Wert SE, Mucenski ML, Scott WJ & Whitsett JA. (2008). R-spondin 2 is required for normal laryngeal-tracheal, lung and limb morphogenesis. *Development* **135,** 1049-1058.

Chen MK & Badylak SF. (2001). Small bowel tissue engineering using small intestinal submucosa as a scaffold. *J Surg Res* **99,** 352-358.

Chu S & Montrose MH. (1995). Extracellular pH regulation in microdomains of colonic crypts: effects of short-chain fatty acids. *Proc Natl Acad Sci U S A* **92,** 3303-3307.

de la Fuente SG, Gottfried MR, Lawson DC, Harris MB, Mantyh CR & Pappas TN. (2003). Evaluation of porcine-derived small intestine submucosa as a biodegradable graft for gastrointestinal healing. *J Gastrointest Surg* **7,** 96-101.

Doede T, Bondartschuk M, Joerck C, Schulze E & Goernig M. (2009). Unsuccessful alloplastic esophageal replacement with porcine small intestinal submucosa. *Artif Organs* **33,** 328-333.

Feng R, Aihara E, Kenny S, Yang L, Li J, Varro A, Montrose MH, Shroyer NF, Wang TC, Shivdasani RA & Zavros Y. (2014). Indian Hedgehog Mediates Gastrin-Induced Proliferation in Stomach of Adult Mice. *Gastroenterology* **In Press**.

Hodde J, Janis A, Ernst D, Zopf D, Sherman D & Johnson C. (2007). Effects of sterilization on an extracellular matrix scaffold: part I. Composition and matrix architecture. *J Mater Sci Mater Med* **18,** 537-543.

Hoeppner J, Crnogorac V, Marjanovic G, Jüttner E, Keck T, Weiser HF & Hopt UT. (2009). Small intestinal submucosa for reinforcement of colonic anastomosis. *Int J Colorectal Dis* **24,** 543-550.

Jaks V, Barker N, Kasper M, van Es JH, Snippert HJ, Clevers H & Toftgård R. (2008). Lgr5 marks cycling, yet long-lived, hair follicle stem cells. *Nat Genet* **40,** 1291-1299.

Karam SM & Leblond CP. (1993). Dynamics of epithelial cells in the corpus of the mouse stomach. I. Identification of proliferative cell types and pinpointing of the stem cell. *Anat Rec* **236,** 259-279.

Khurana SS, Riehl TE, Moore BD, Fassan M, Rugge M, Romero-Gallo J, Noto J, Peek RMJ, Stenson WF & Mills JC. (2013). The hyaluronic acid receptor CD44 coordinates normal and metaplastic gastric epithelial progenitor cell proliferation. *J Biol Chem* **288,** 16085-16097.

Kikuchi M, Nagata H, Watanabe N, Watanabe H, Tatemichi M & Hibi T. (2010). Altered expression of a putative progenitor cell marker DCAMKL1 in the rat gastric mucosa in regeneration, metaplasia and dysplasia. *BMC Gastroenterol* **10,** 65.

Kim BM, Buchner G, Miletich I, Sharpe PT & Shivdasani RA. (2005). The stomach mesenchymal transcription factor Barx1 specifies gastric epithelial identity through inhibition of transient Wnt signaling. *Dev Cell* **8,** 611-622.

Kim BM, Woo J, C. K & R.A. S. (2011). Regulation of mouse stomach development and Barx1 expression by specific microRNAs. *Development* **138,** 1081-1086.

Lambrecht NW, Yakubov I, Scott D & Sachs G. (2005). Identification of the K efflux channel coupled to the gastric H-K-ATPase during acid secretion. *Physiol Genomics* **21,** 81-91.

Lee M, Chang PC & Dunn JC. (2008). Evaluation of small intestinal submucosa as scaffolds for intestinal tissue engineering. *J Surg Res* **147,** 168-171.

Livak K & Schmittgen T. (2001). Analysis of relative gene expression data using real-time quantitative PCR and the 2(-Delta Delta C(T)) Method. *Methods* **25,** 402-408.

McDevitt CA, Wildey GM & Cutrone RM. (2003). Transforming growth factor-beta1 in a sterilized tissue derived from the pig small intestine submucosa. *J Biomed Mater Res A* **67,** 637-640.

Mills JC & Shivdasani RA. (2011). Gastric epithelial stem cells. *Gastroenterology* **140,** 412-424.

Moskaluk CA, Zhang H, Powell SM, Cerilli LA, Hampton GM & Frierson HFJ. (2003). Cdx2 protein expression in normal and malignant human tissues: an immunohistochemical survey using tissue microarrays. *Mod Pathol* **16,** 913-919.

Nakatsu H, Ueno T, Oga A, Nakao M, Nishimura T, Kobayashi S & Oka M. (2013). Influence of mesenchymal stem cells on stomach tissue engineering using small intestinal submucosa. *J Tissue Eng Regen Med* **In Press**.

Nishimura T, Ueno T, Nakatsu H, Oga A, Kobayashi S & Oka M. (2010). In vivo motility evaluation of the grafted gastric wall with small intestinal submucosa. *Tissue Eng Part A* **16,** 1761-1768.

Nozaki K OM, Williams JA, Lafleur BJ, Ng V, Drapkin RI, Mills JC, Konieczny SF, Nomura S, Goldenring JR. (2008). A molecular signature of gastric metaplasia arising in response to acute parietal cell loss. *Gastroenterology* **134,** 511-522.

Nyqvist D, Mattsson G, Köhler M, Lev-Ram V, Andersson A, Carlsson PO, Nordin A, Berggren PO & Jansson L. (2005). Pancreatic islet function in a transgenic mouse expressing fluorescent protein. *J Endocrinol* **186,** 333-341.

Prinz C, Kajimura M, Scott DR, Mercier F, Helander HF & Sachs G. (1993). Histamine secretion from rat enterochromaffinlike cells. *Gastroenterology* **105,** 449-461.

Qin HH & Dunn JC. (2011). Small intestinal submucosa seeded with intestinal smooth muscle cells in a rodent jejunal interposition model. *J Surg Res* **171,** 21-26.

Quante M, Marrache F, Goldenring JR & Wang TC. (2010). TFF2 mRNA transcript expression marks a gland progenitor cell of the gastric oxyntic mucosa. *Gastroenterology* **139,** 2018-2027.

Schumacher MA, Feng R, Aihara E, Engevik AC, Montrose MH, Ottemann KM & Zavros Y. (2014). Helicobacter pylori-induced Sonic Hedgehog expression is regulated by NFkB pathway activation: The use of a novel in vitro model to study epithelial response to infection. . *Helicobacter*.

Shaulian E, Zauberman A, Ginsberg D & Oren M. (1992). Identification of a minimal transforming domain of p53: negative dominance through abrogation of sequence-specific DNA binding. *Mol Cell Biol* **12,** 5581-5592.

Stange DE, Koo BK, Huch M, Sibbel G, Basak O, Lyubimova A, Kujala P, Bartfeld S, Koster J, Geahlen JH, Peters PJ, van Es JH, van de Wetering M, Mills JC & Clevers H. (2013). Differentiated Troy+ chief cells act as reserve stem cells to generate all lineages of the stomach epithelium. *Cell* **155,** 357-368.

Ueno T, de la Fuente SG, Abdel-Wahab OI, Takahashi T, Gottfried M, Harris MB, Tatewaki M, Uemura K, Lawson DC, Mantyh CR & Pappas TN. (2007a). Functional evaluation of the grafted wall with porcine-derived small intestinal submucosa (SIS) to a stomach defect in rats. *Surgery* **142,** 376-383.

Ueno T, Oga A, Takahashi T & Pappas TN. (2007b). Small intestinal submucosa (SIS) in the repair of a cecal wound in unprepared bowel in rats. *J Gastrointest Surg* **11,** 918-922.

Voytik-Harbin SL, Brightman AO, Kraine MR, Waisner B & Badylak SF. (1997). Identification of extractable growth factors from small intestinal submucosa. *J Cell Biochem* **67,** 478-491.

Waldum HL, Arnestad JS, Brenna E, Eide I, Syversen U & Sandvik AK. (1996). Marked increase in gastric acid secretory capacity after omeprazole treatment. *Gut* **39,** 649-653.

Wallmark B, Sachs G, Mardh S & Fellenius E. (1983). Inhibition of gastric (H+ + K+)-ATPase by the substituted benzimidazole, picoprazole. *Biochem Biophys Acta* **728,** 31-38.

Wang ZQ, Watanabe Y & Toki A. (2003). Experimental assessment of small intestinal submucosa as a small bowel graft in a rat model. *J Pediatr Surg* **38,** 1596-1601.

Xue L, Aihara E, Wang TC & Montrose MH. (2011). Trefoil factor 2 requires Na/H exchanger 2 activity to enhance mouse gastric epithelial repair. *J Biol Chem* **286,** 38375-38382.

Yui S, Nakamura T, Sato T, Nemoto Y, Mizutani T, Zheng X, Ichinose S, Nagaishi T, Okamoto R, Tsuchiya K, Clevers H & Watanabe M. (2012). Functional engraftment of colon epithelium expanded in vitro from a single adult Lgr5□ stem cell. *Nat Med* **18,** 618-623.

Zhang ZW, Dorrell N, Wren BW & Farthingt MJ. (2002). Helicobacter pylori adherence to gastric epithelial cells: a role for non-adhesin virulence genes. *J Med Microbiol* **51,** 495-502.

Figure 1

Fundic Organoid Development

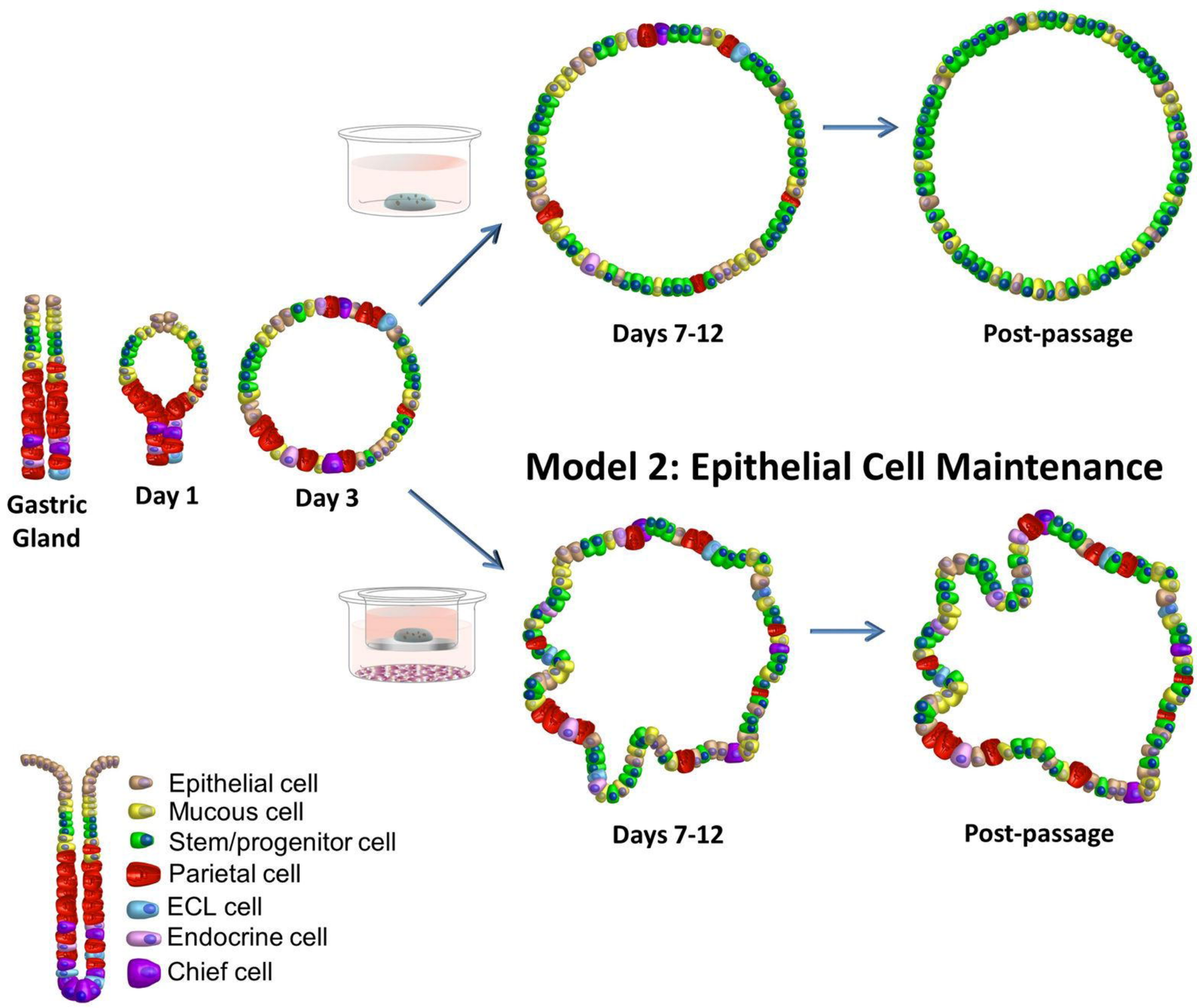

Assays (Initial 7-12 Days Culture)

- Physiological Function
- Gastric Disease

Assays (Post-passage: >12 days)

- Stem Cell Biology
- Tissue Repair/Regeneration

Assays

- Physiological Function
- Gastric Disease
- Epithelial Cell Biology
- Tissue Repair/Regeneration

Figure 2

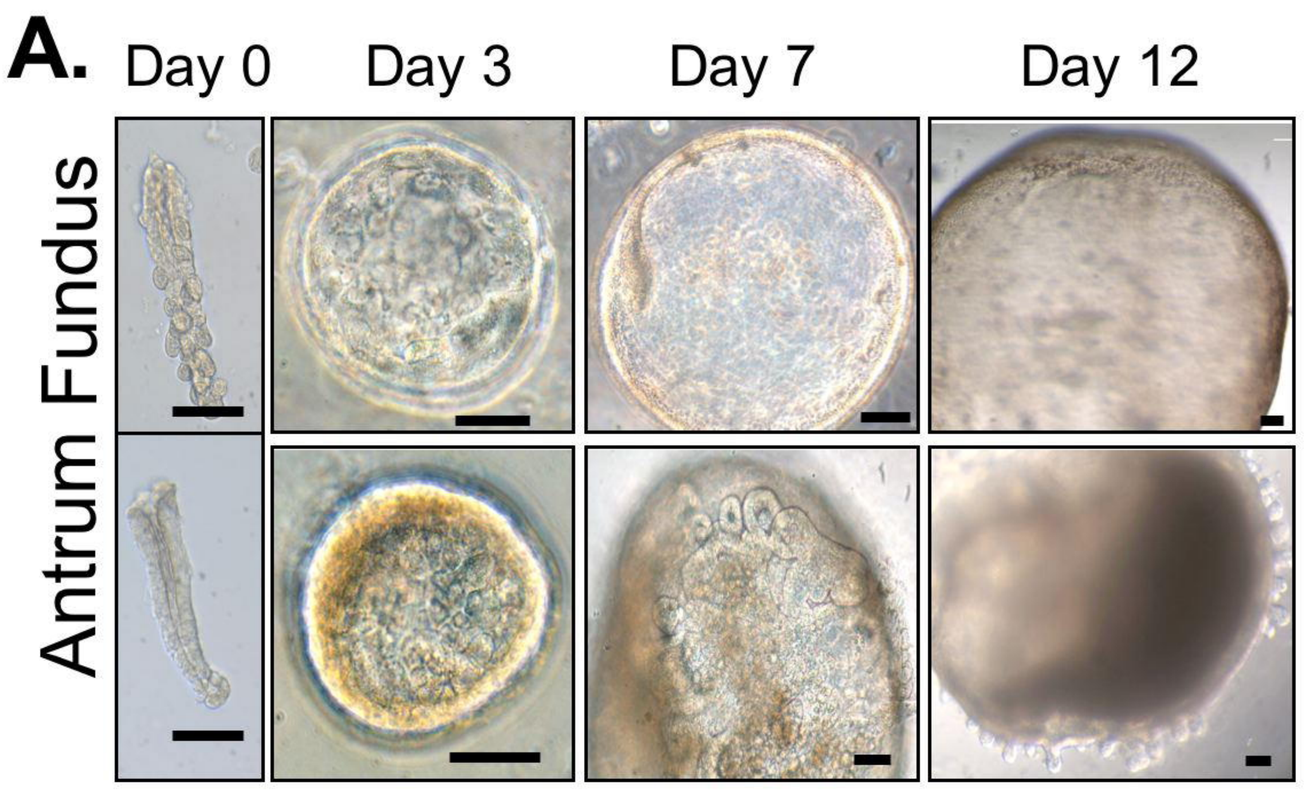
A.
Day 0
Day 3
Day 7
Day 12
Antrum
Fundus

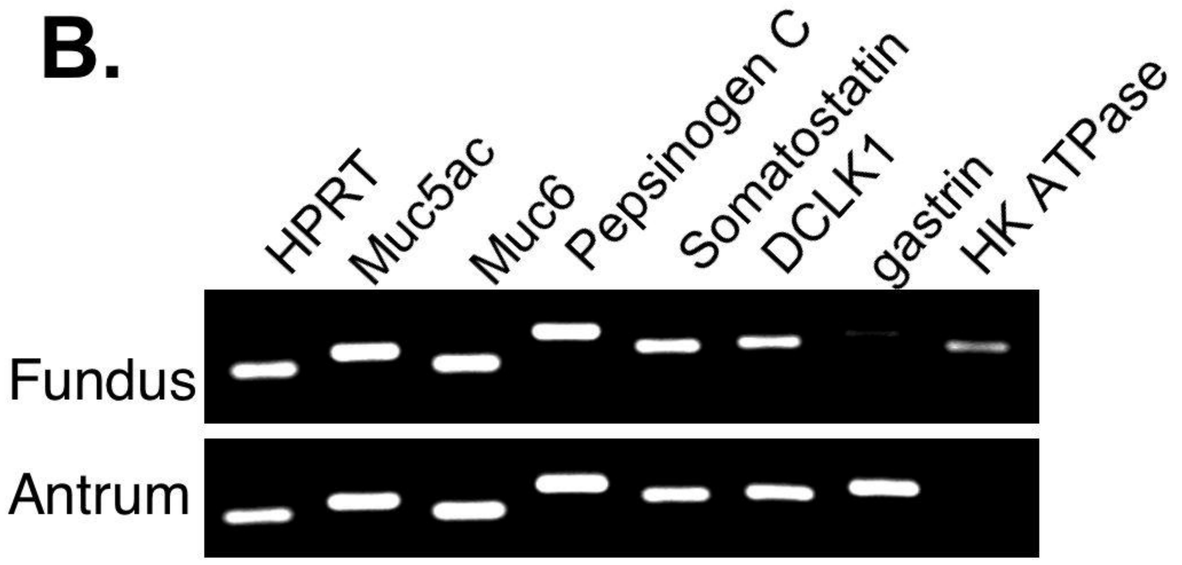
B.
HPRT
Muc5ac
Muc6
Pepsinogen C
Somatostatin
DCLK1
gastrin
HK ATPase
Fundus
Antrum

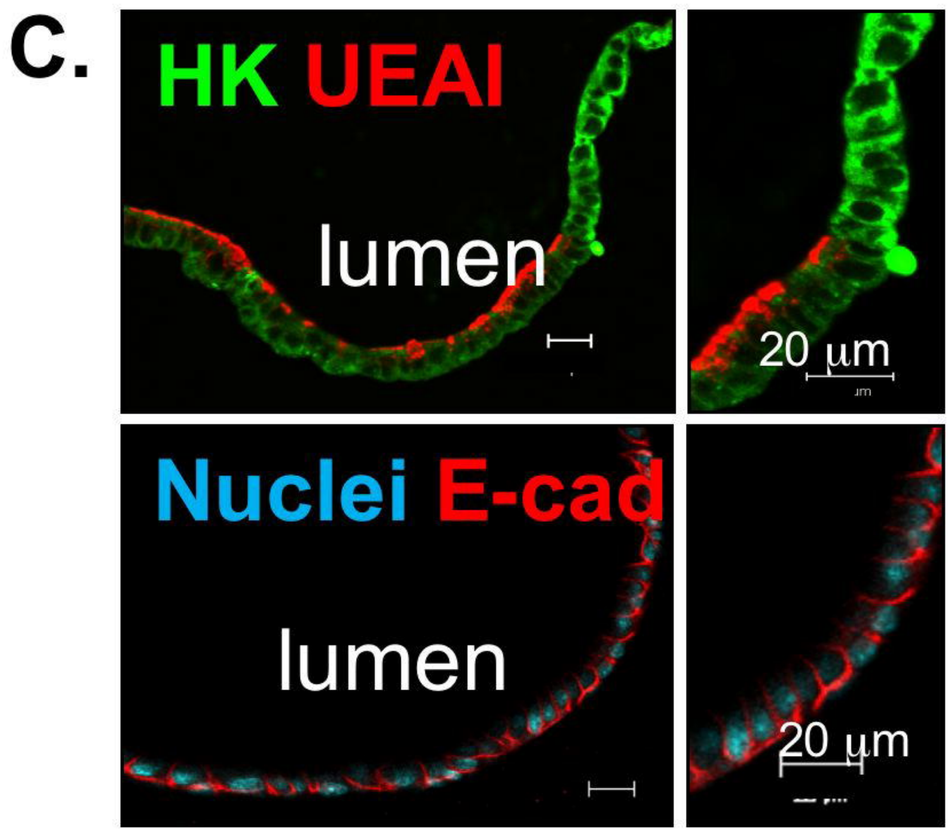
C.
HK UEAI
lumen
20 μm
Nuclei E-cad
lumen
20 μm

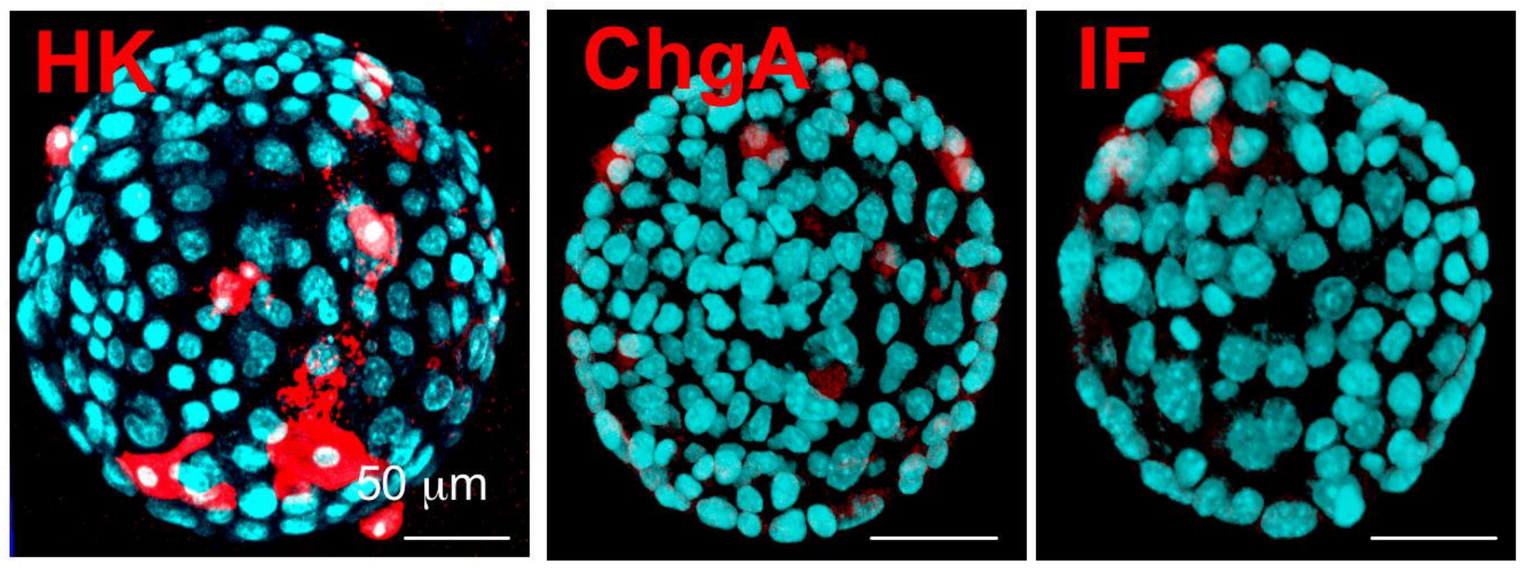
D.
HK
50 μm
ChgA
IF

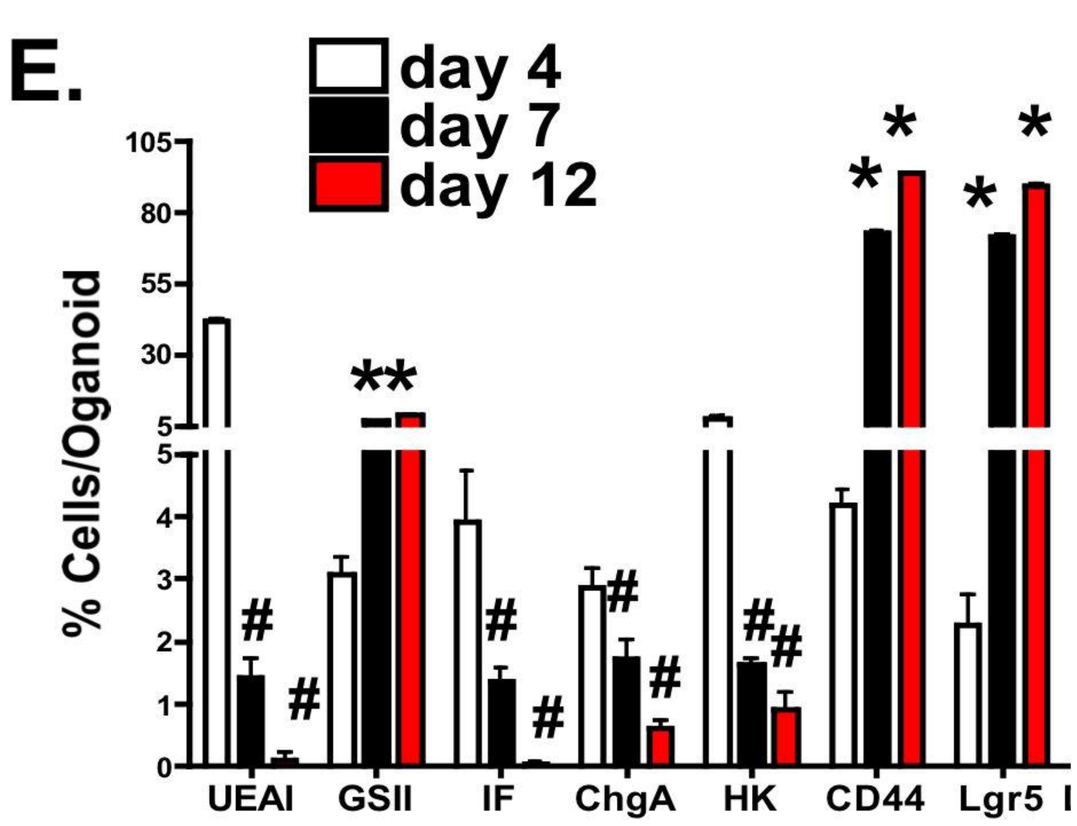
E.
day 4
day 7
day 12
% Cells/Oganoid
UEAI
GSII
IF
ChgA
HK
CD44
Lgr5

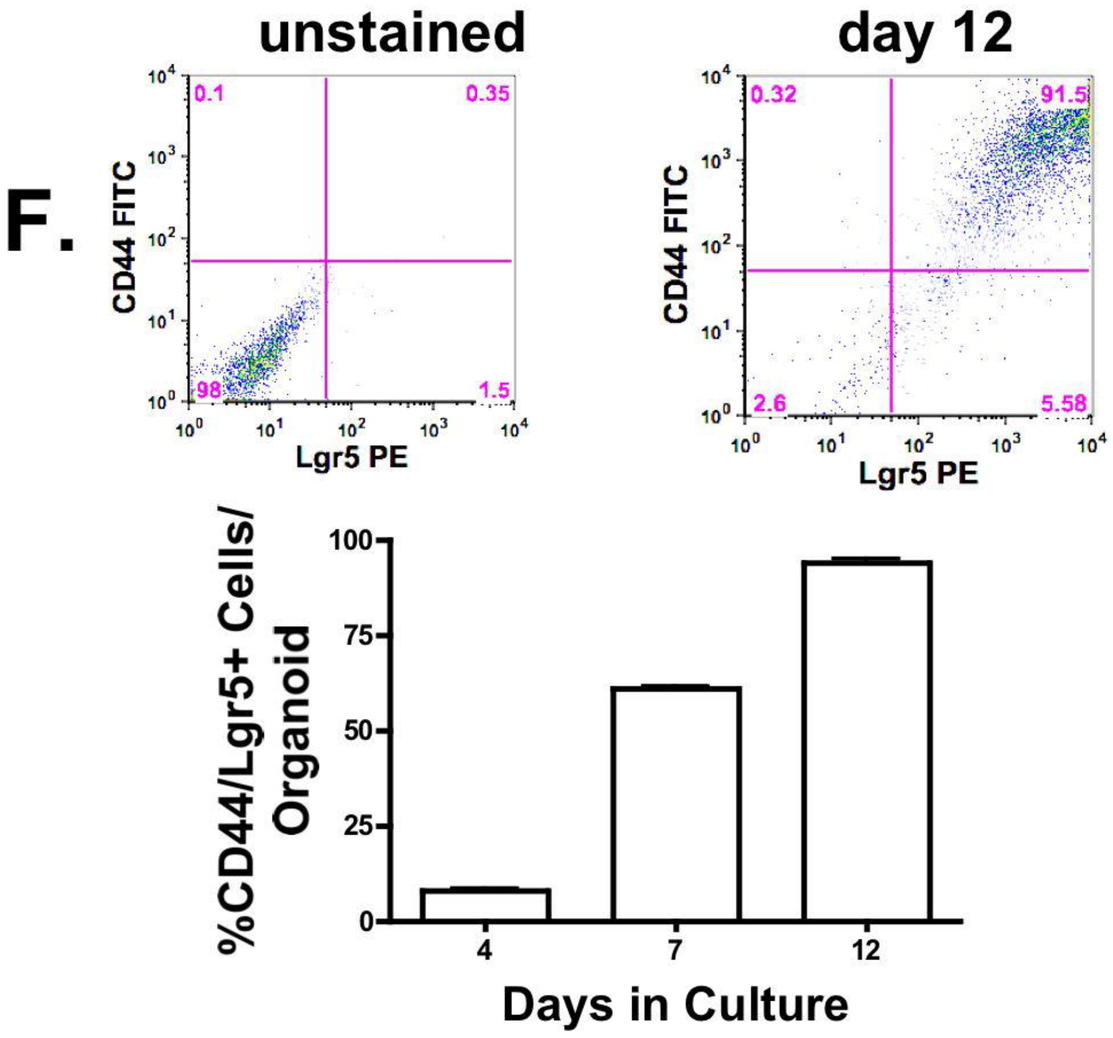
F.
unstained
day 12
CD44 FITC
Lgr5 PE
0.1
0.35
98
1.5
0.32
91.5
2.6
5.58
%CD44/Lgr5+ Cells/ Organoid
Days in Culture

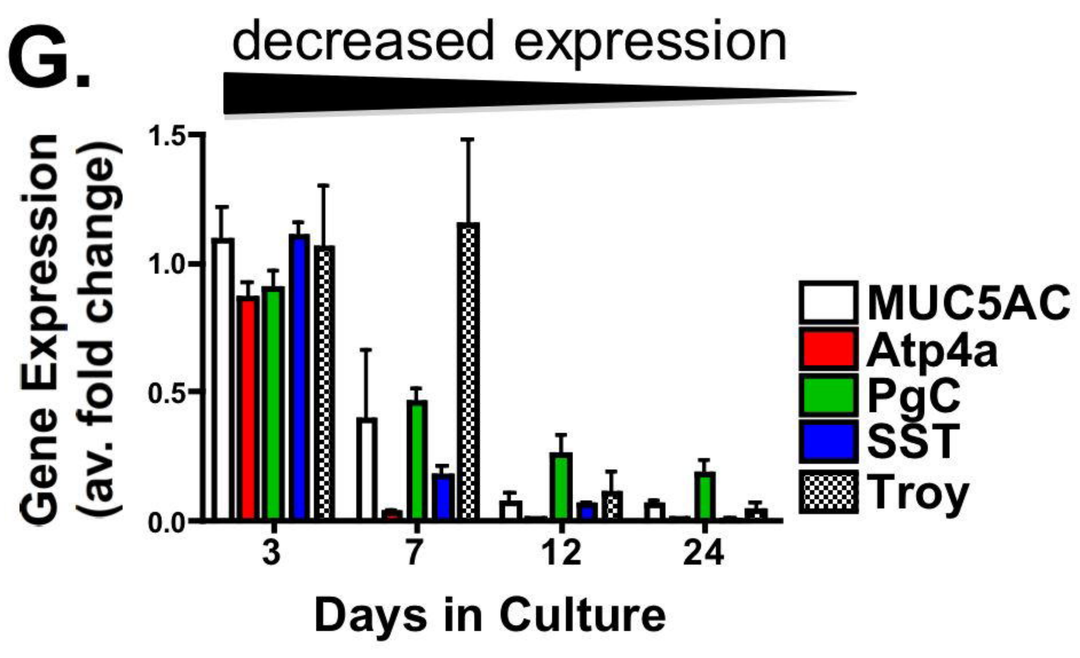
G.
decreased expression
Gene Expression (av. fold change)
MUC5AC
Atp4a
PgC
SST
Troy
Days in Culture

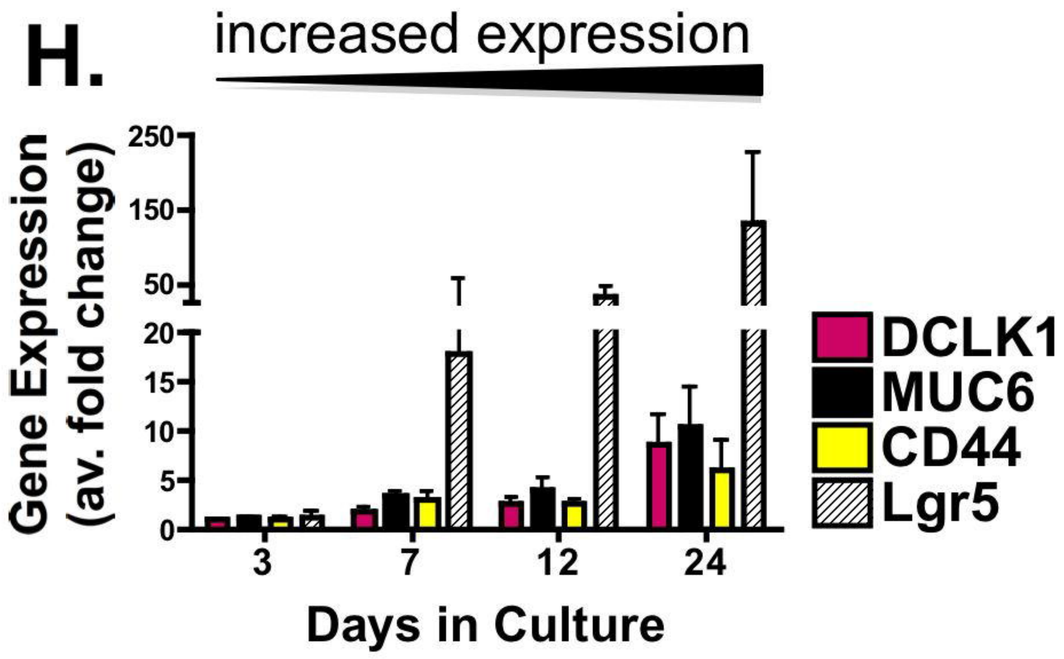
H.
increased expression
Gene Expression (av. fold change)
DCLK1
MUC6
CD44
Lgr5
Days in Culture

Figure 3

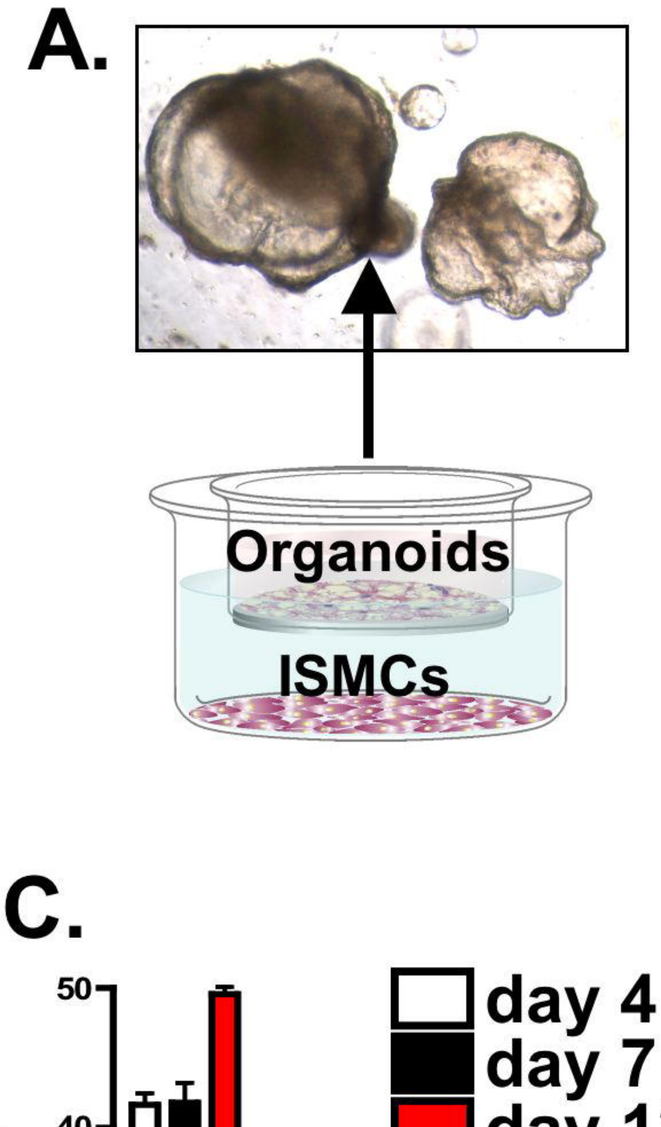
A.
Organoids
ISMCs

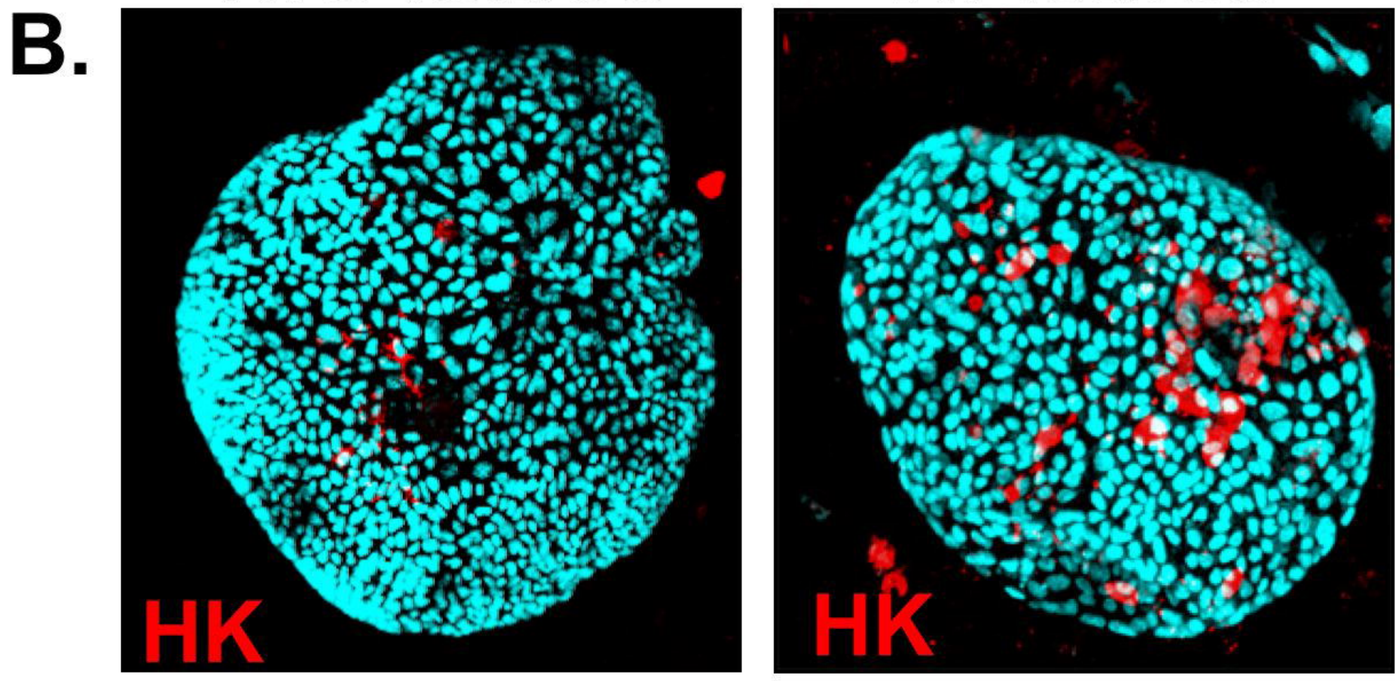
B.
W/O ISMCs
W/ ISMCs
HK
HK

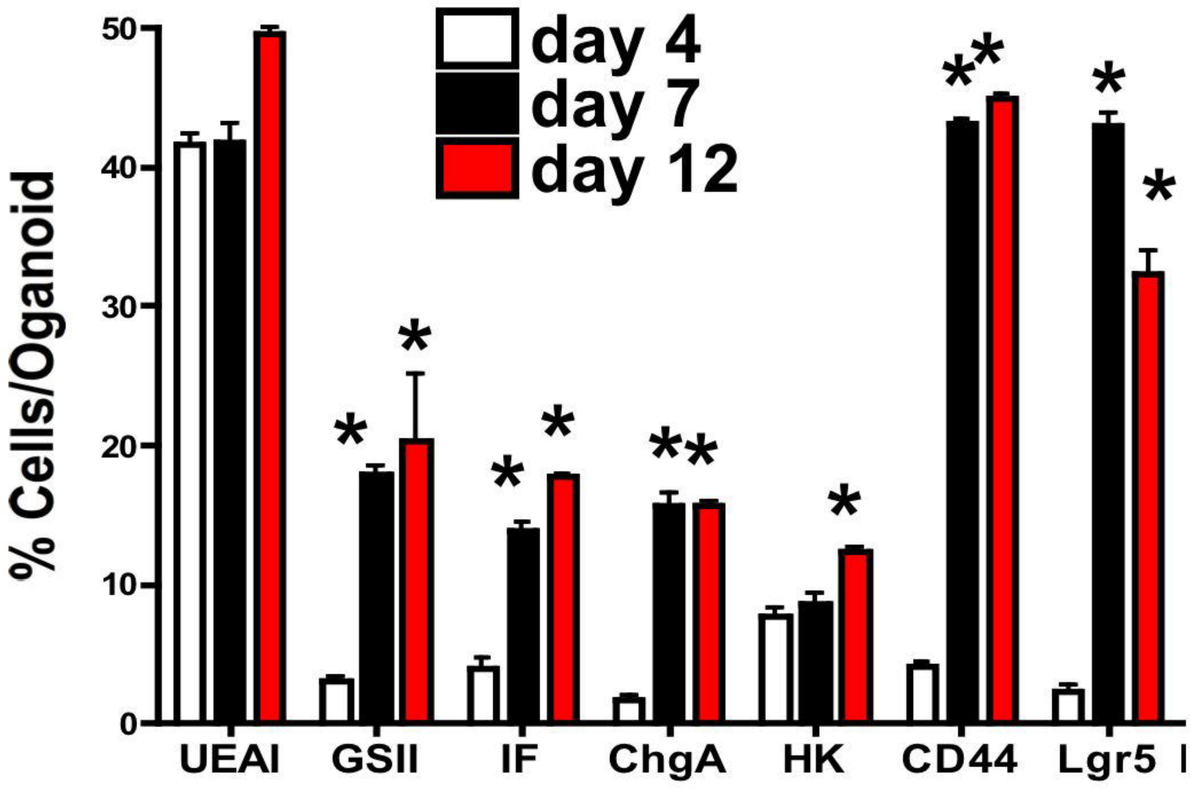
C.
day 4
day 7
day 12
% Cells/Oganoid
UEAl
GSII
IF
ChgA
HK
CD44
Lgr5

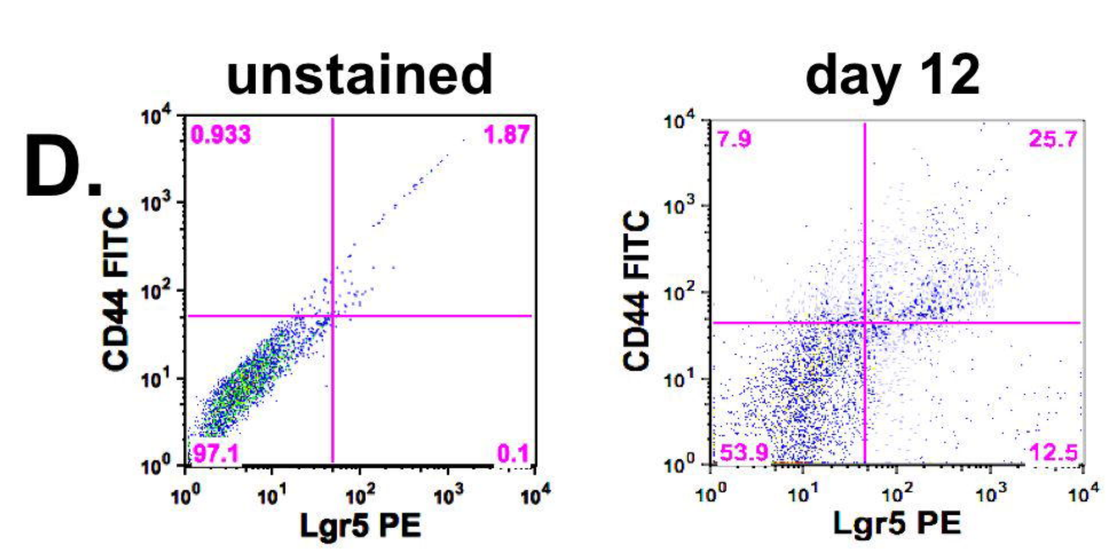
D.
unstained
day 12
CD44 FITC
Lgr5 PE
0.933
1.87
97.1
0.1
7.9
25.7
53.9
12.5
%CD44/Lgr5+ Cells/ Organoid
Days in Culture

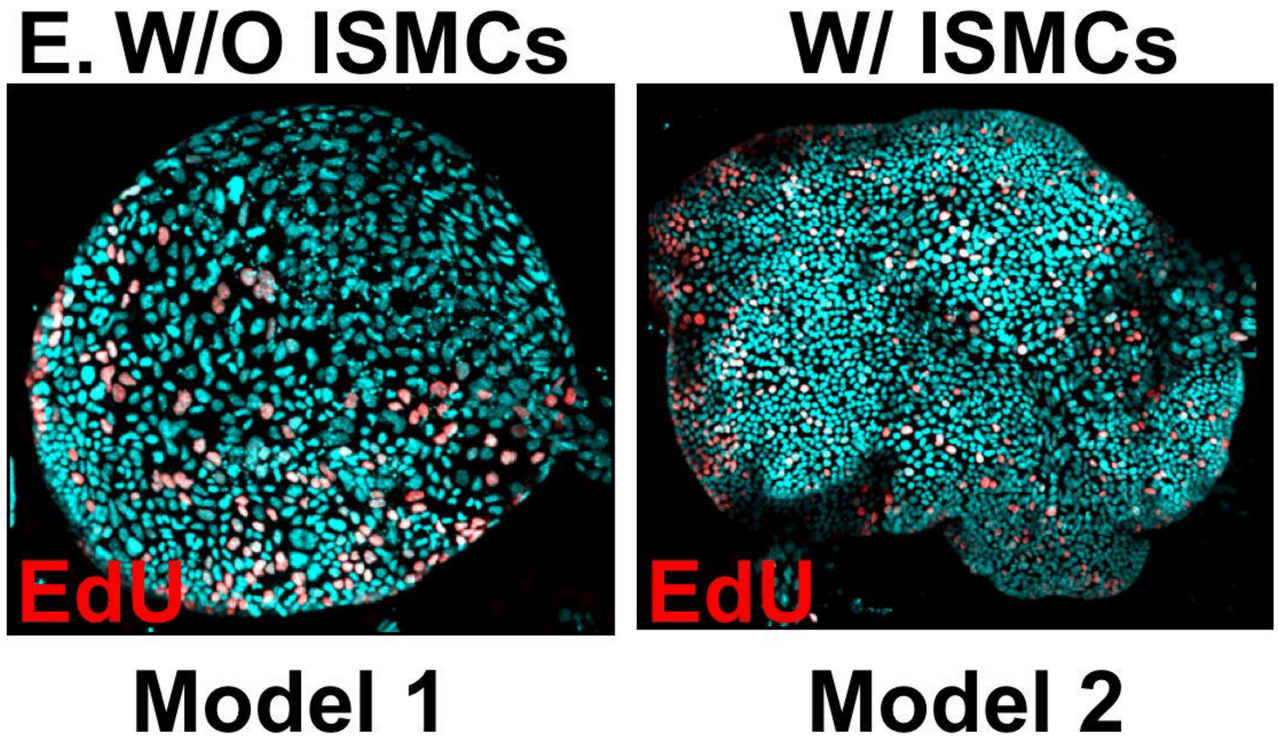
E. W/O ISMCs
W/ ISMCs
EdU
EdU
Model 1
Model 2

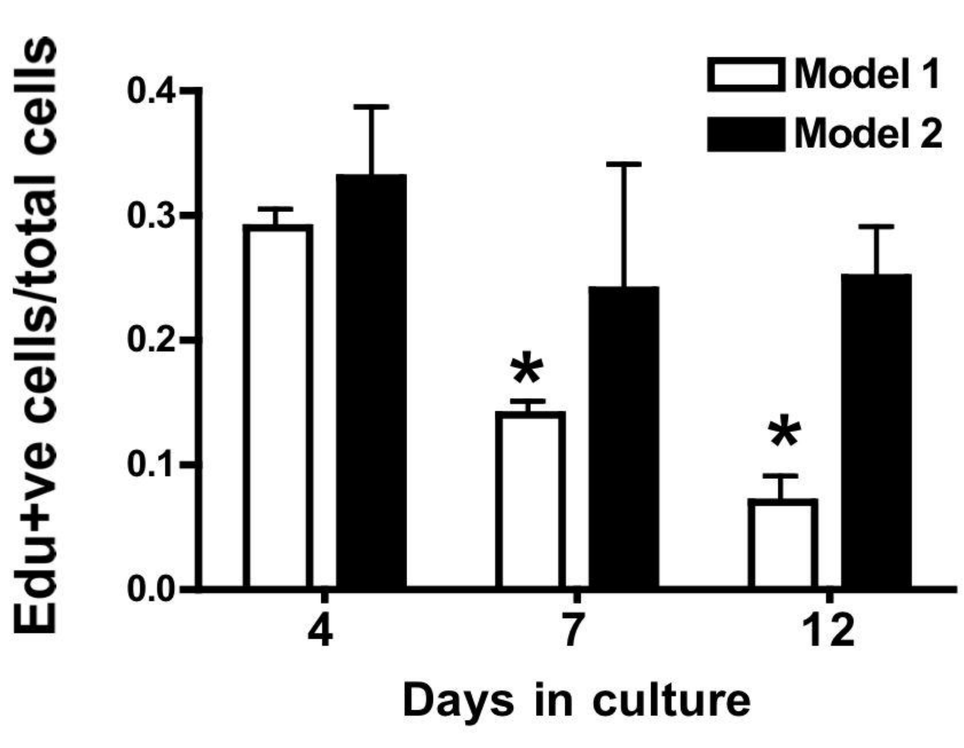
F.
Model 1
Model 2
Edu+ve cells/total cells
Days in culture

Figure 4

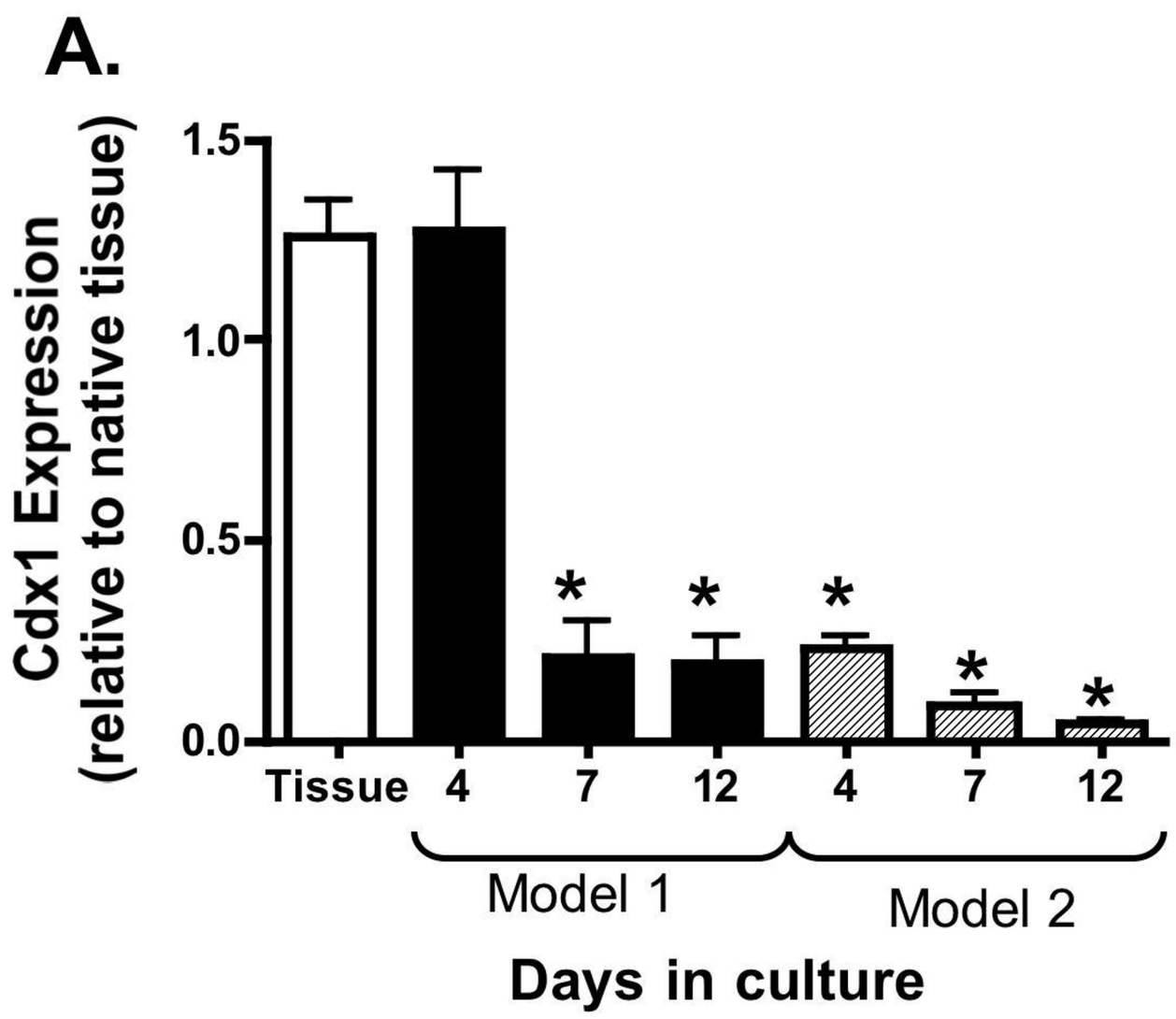
A.
Cdx1 Expression
(relative to native tissue)
1.5
1.0
0.5
0.0
Tissue
4
7
12
4
7
12
Model 1
Model 2
Days in culture

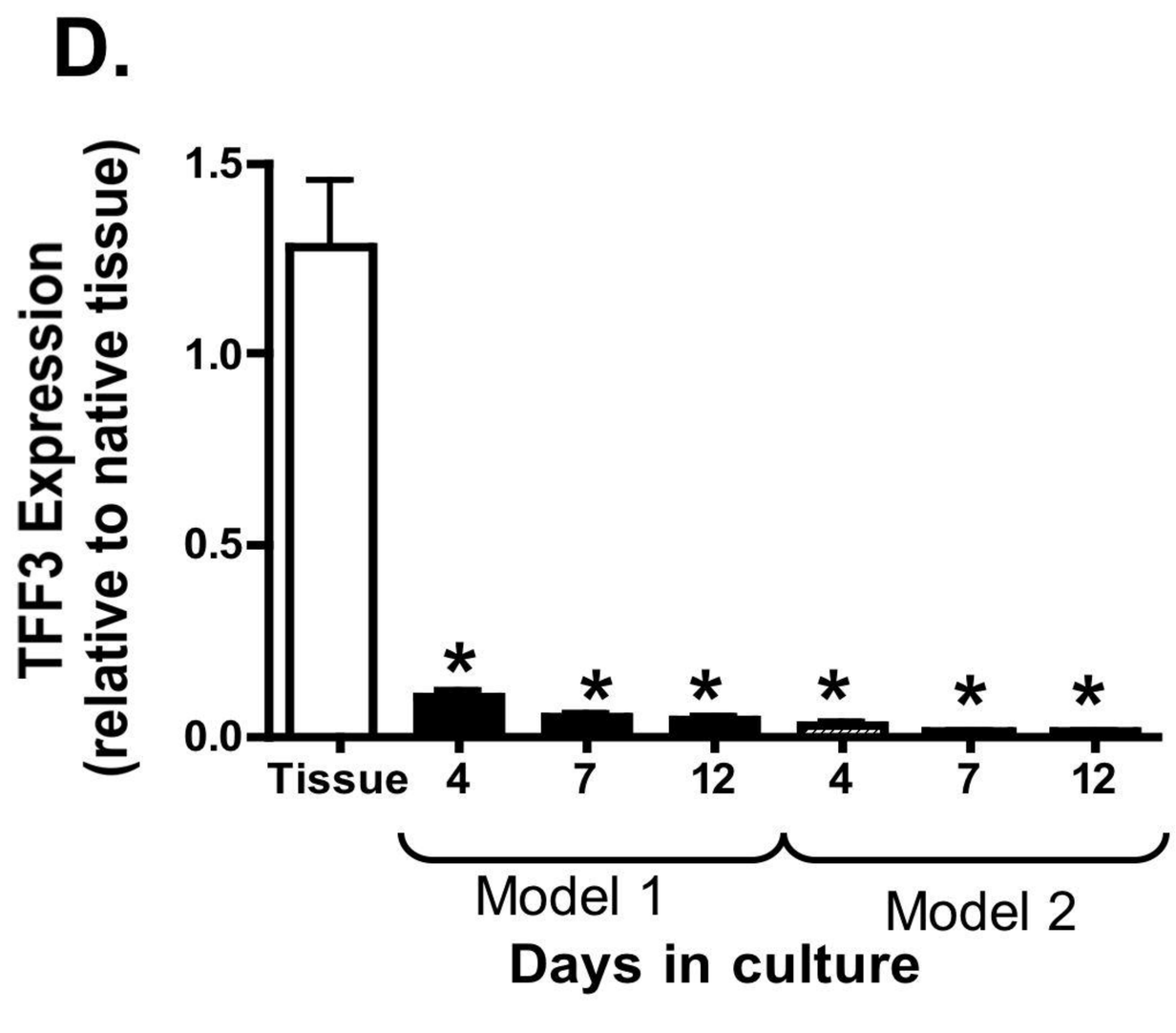
D.
TFF3 Expression
(relative to native tissue)
1.5
1.0
0.5
0.0
Tissue
4
7
12
4
7
12
Model 1
Model 2
Days in culture

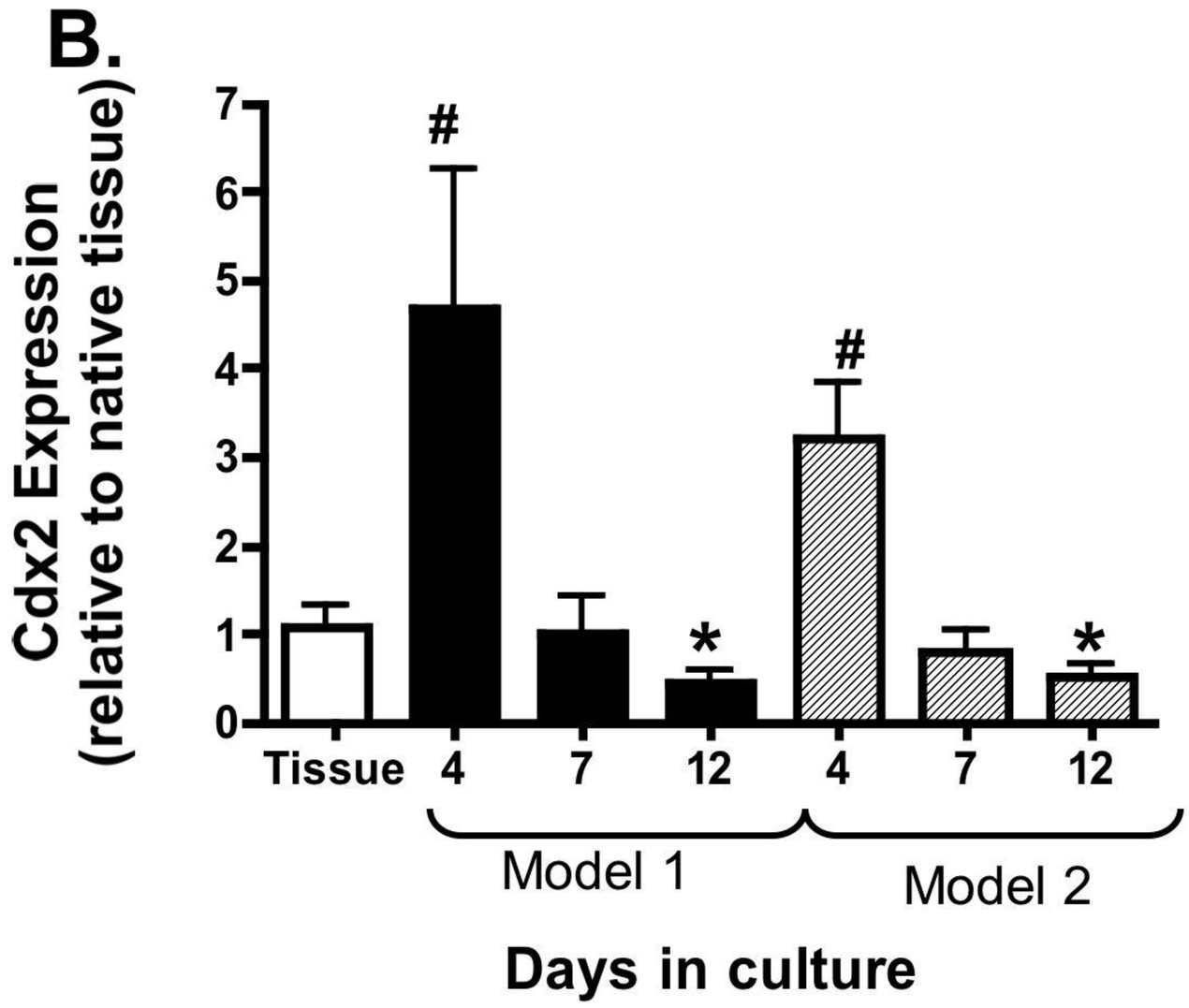
B.
Cdx2 Expression
(relative to native tissue)
7
6
5
4
3
2
1
0
Tissue
4
7
12
4
7
12
Model 1
Model 2
Days in culture

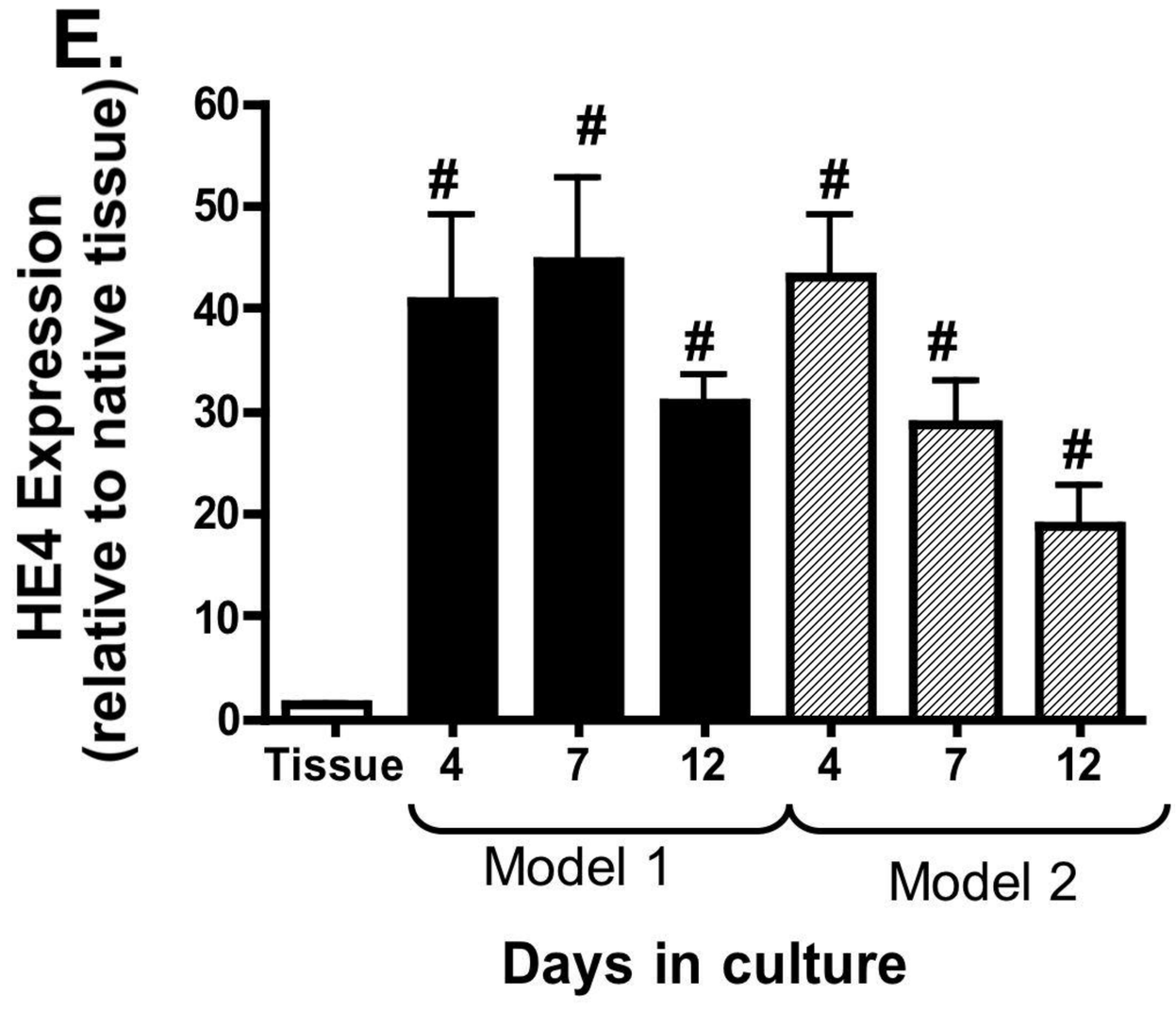
E.
HE4 Expression
(relative to native tissue)
60
50
40
30
20
10
0
Tissue
4
7
12
4
7
12
Model 1
Model 2
Days in culture

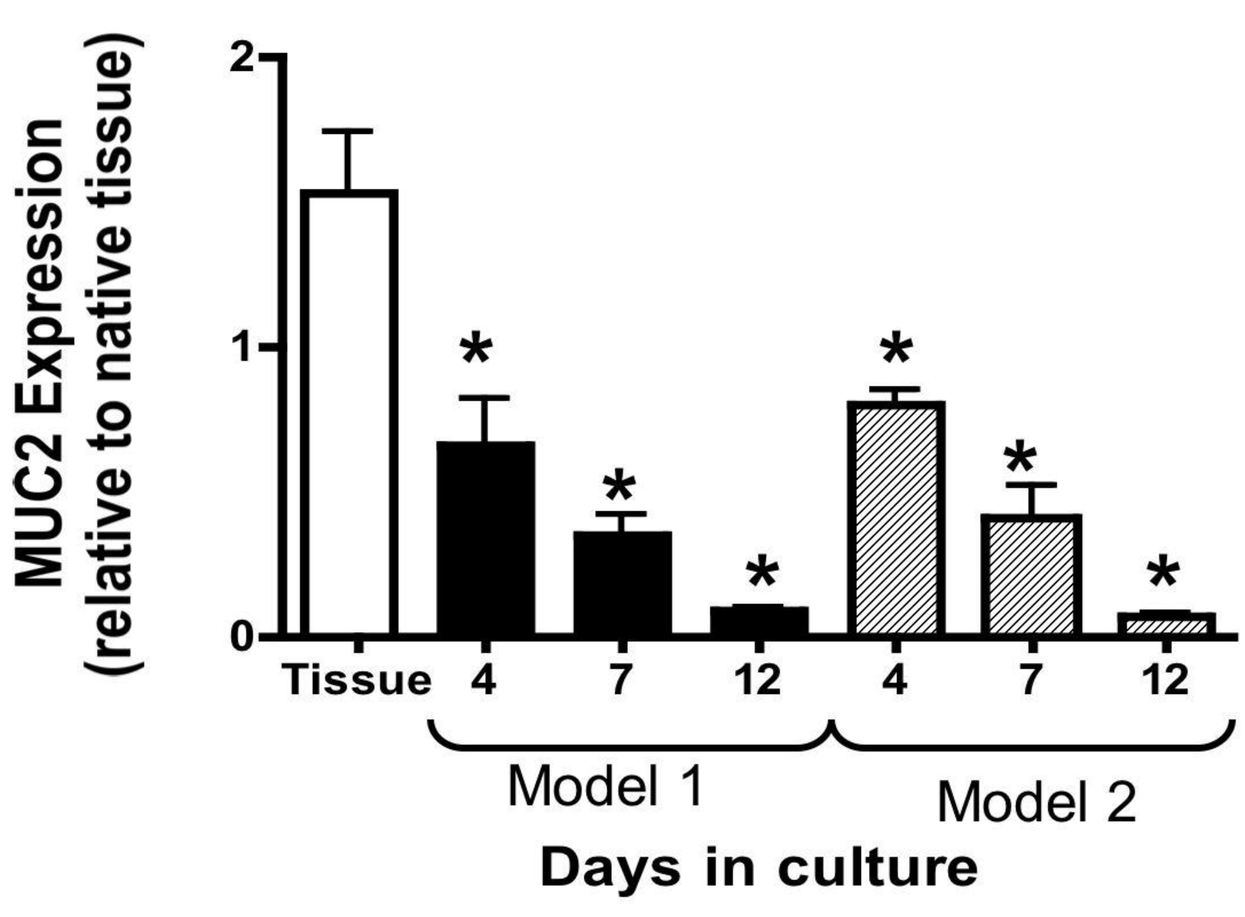
C.
MUC2 Expression
(relative to native tissue)
2
1
0
Tissue
4
7
12
4
7
12
Model 1
Model 2
Days in culture

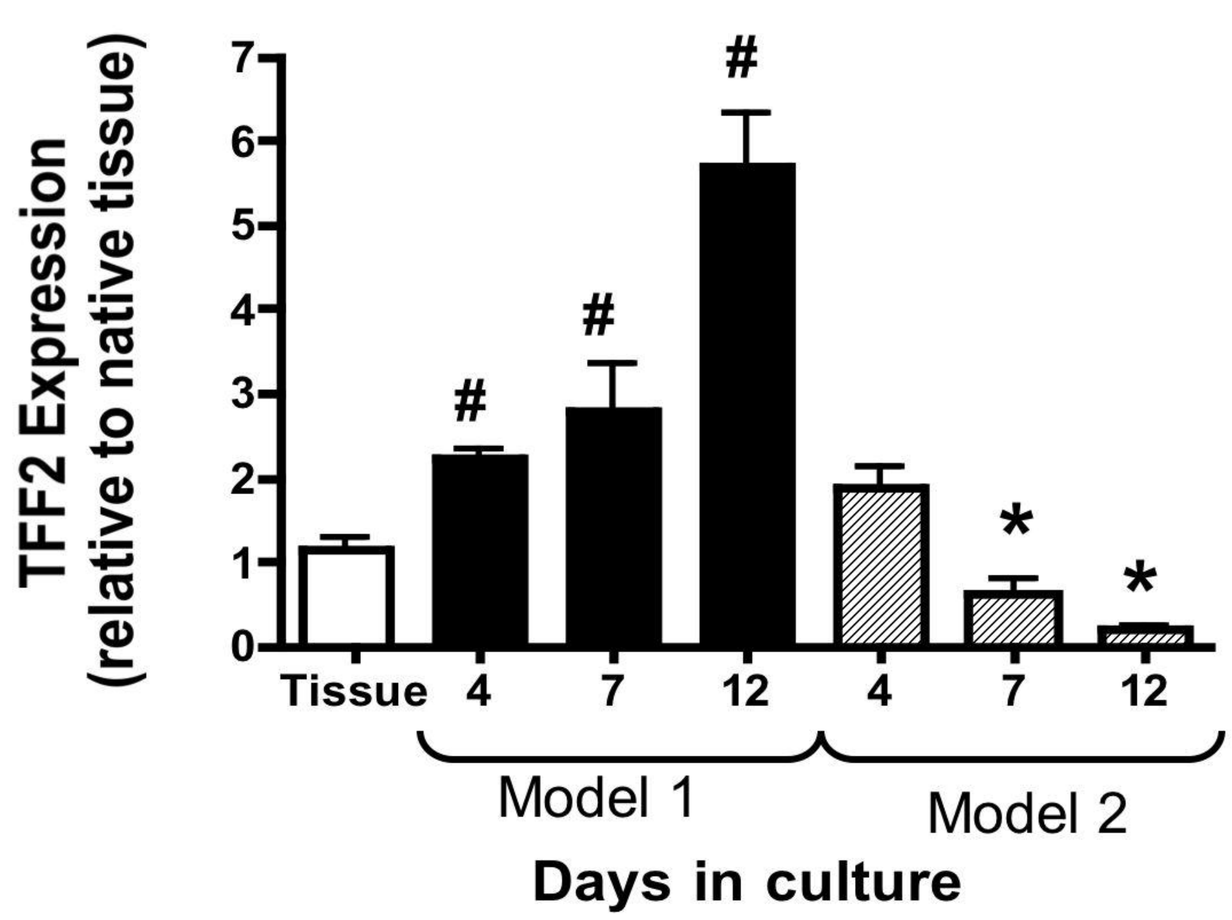
F.
TFF2 Expression
(relative to native tissue)
7
6
5
4
3
2
1
0
Tissue
4
7
12
4
7
12
Model 1
Model 2
Days in culture

Figure 5

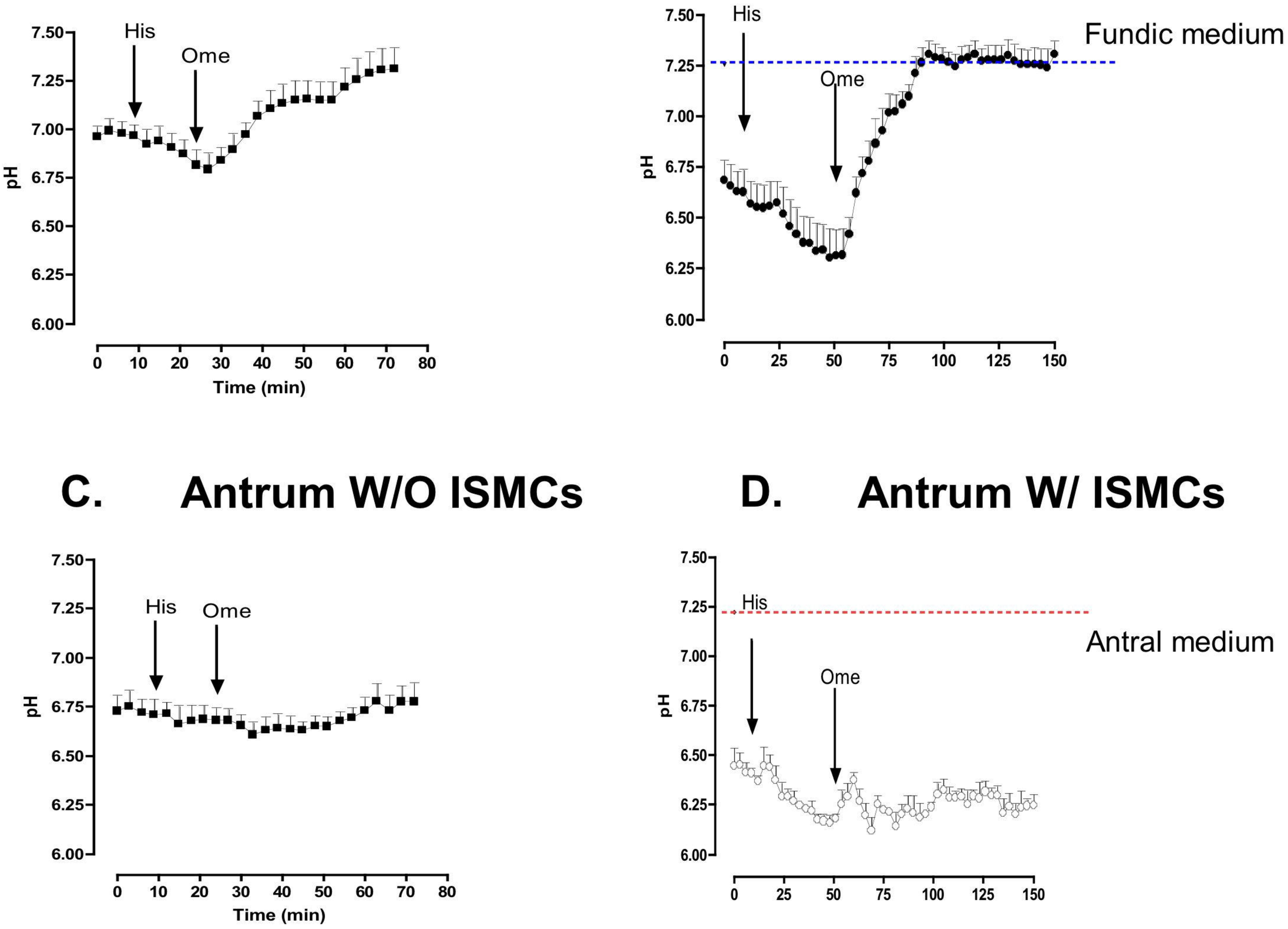
A. Fundus W/O ISMCs
B. Fundus W/ ISMCs
C. Antrum W/O ISMCs
D. Antrum W/ ISMCs
His
Ome
Fundic medium
Antral medium
pH
7.50
7.25
7.00
6.75
6.50
6.25
6.00
0
10
20
30
40
50
60
70
80
25
75
100
125
150
Time (min)

Figure 6

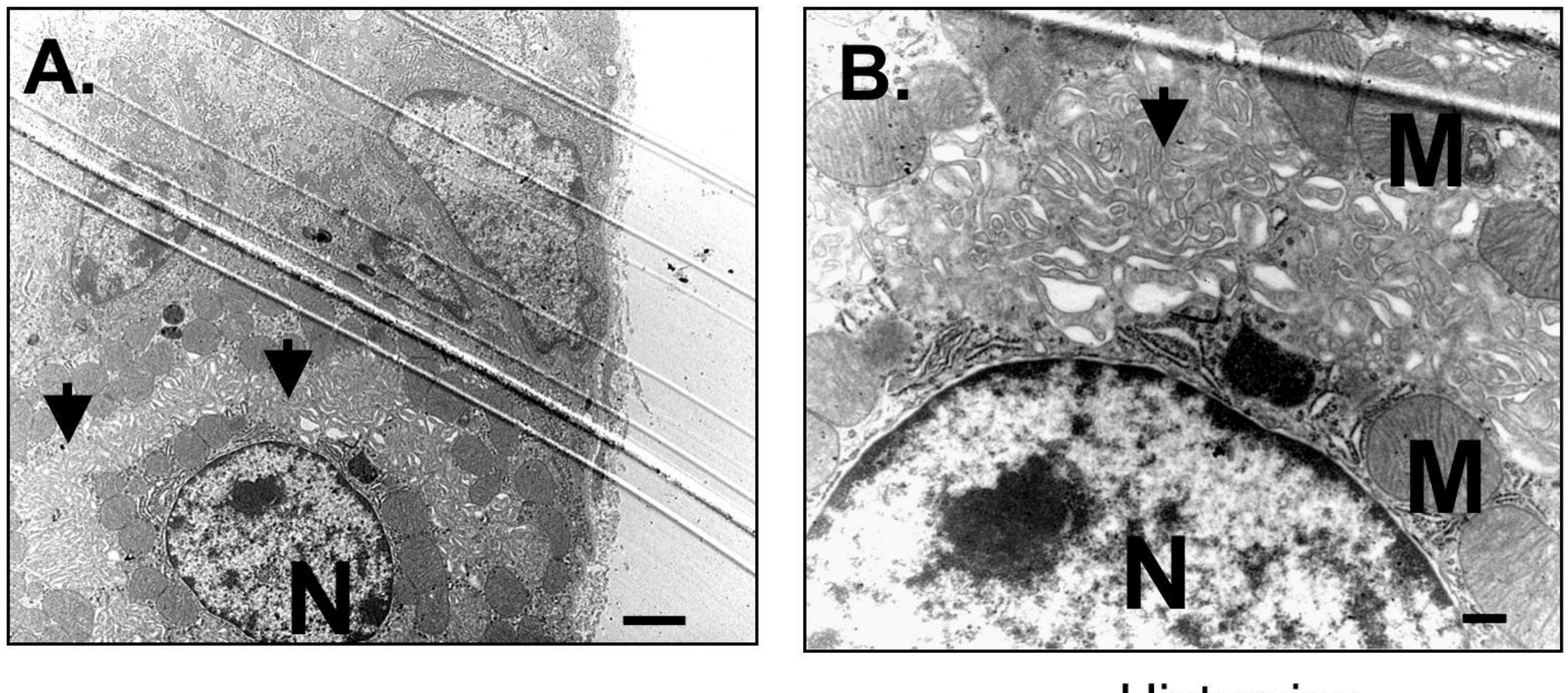
A.
N
B.
M
M
N

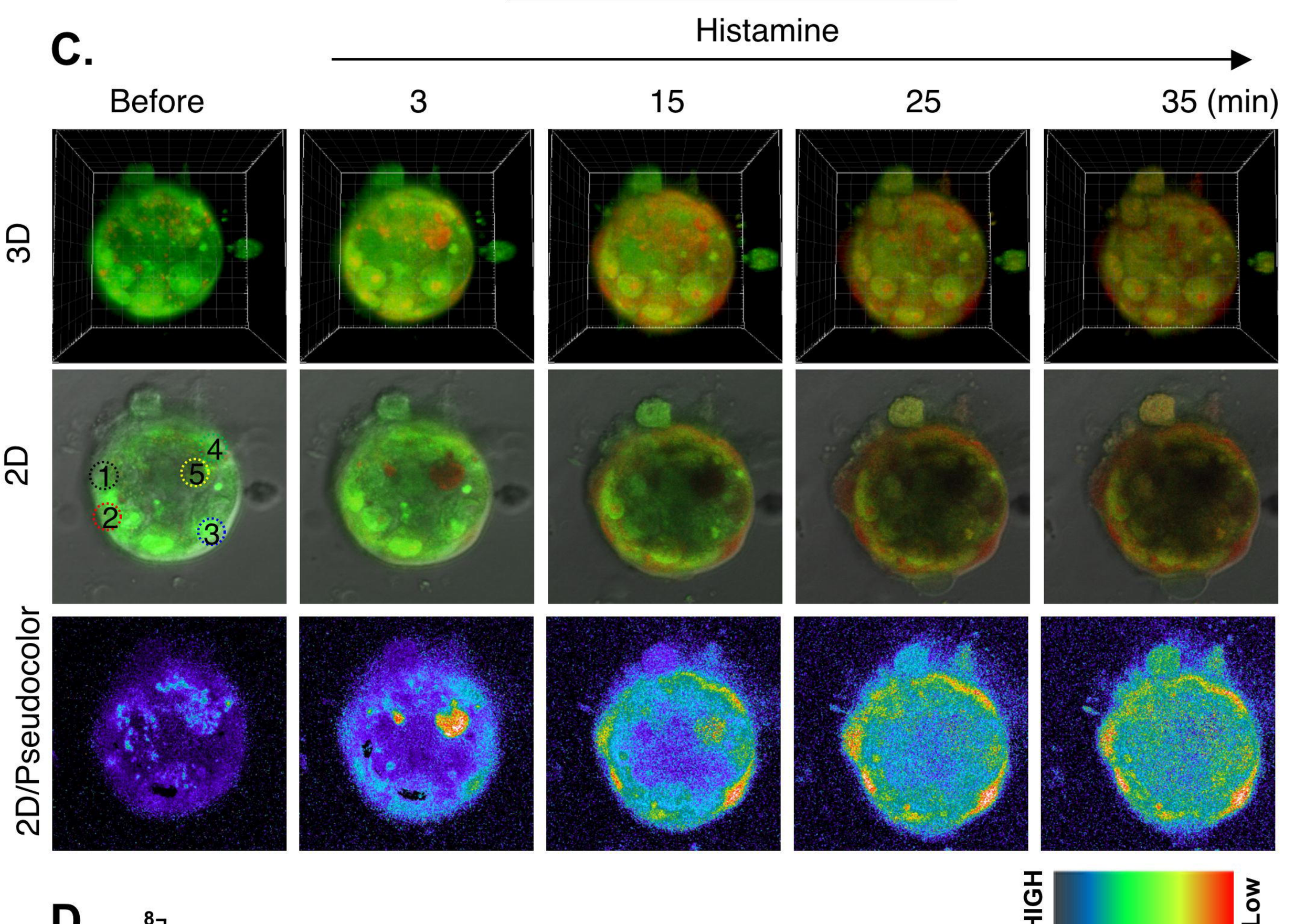
C.
Histamine
Before
3
15
25
35 (min)
3D
2D
2D/Pseudocolor
1
2
3
4
5
HIGH
Low
pH

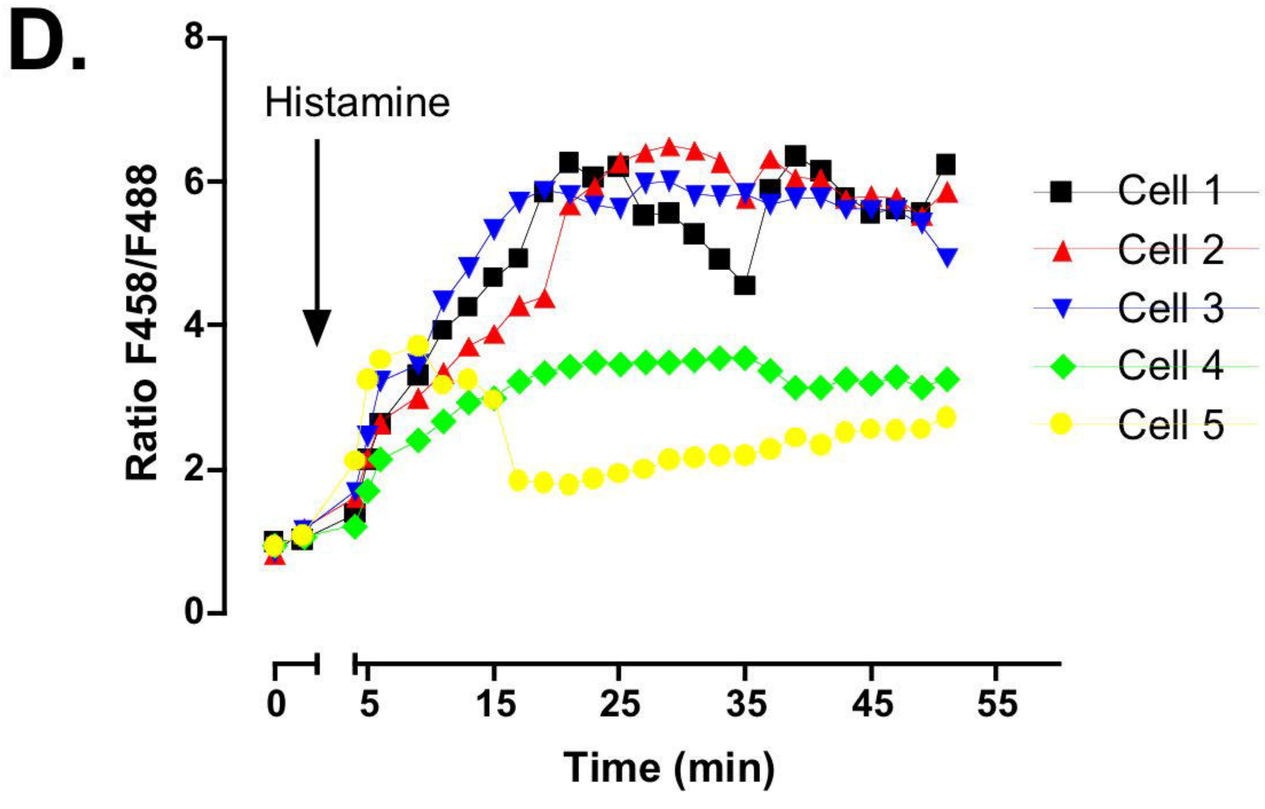
D.
Histamine
Ratio F458/F488
0
2
4
6
8
0
5
15
25
35
45
55
Time (min)
Cell 1
Cell 2
Cell 3
Cell 4
Cell 5

Figure 7

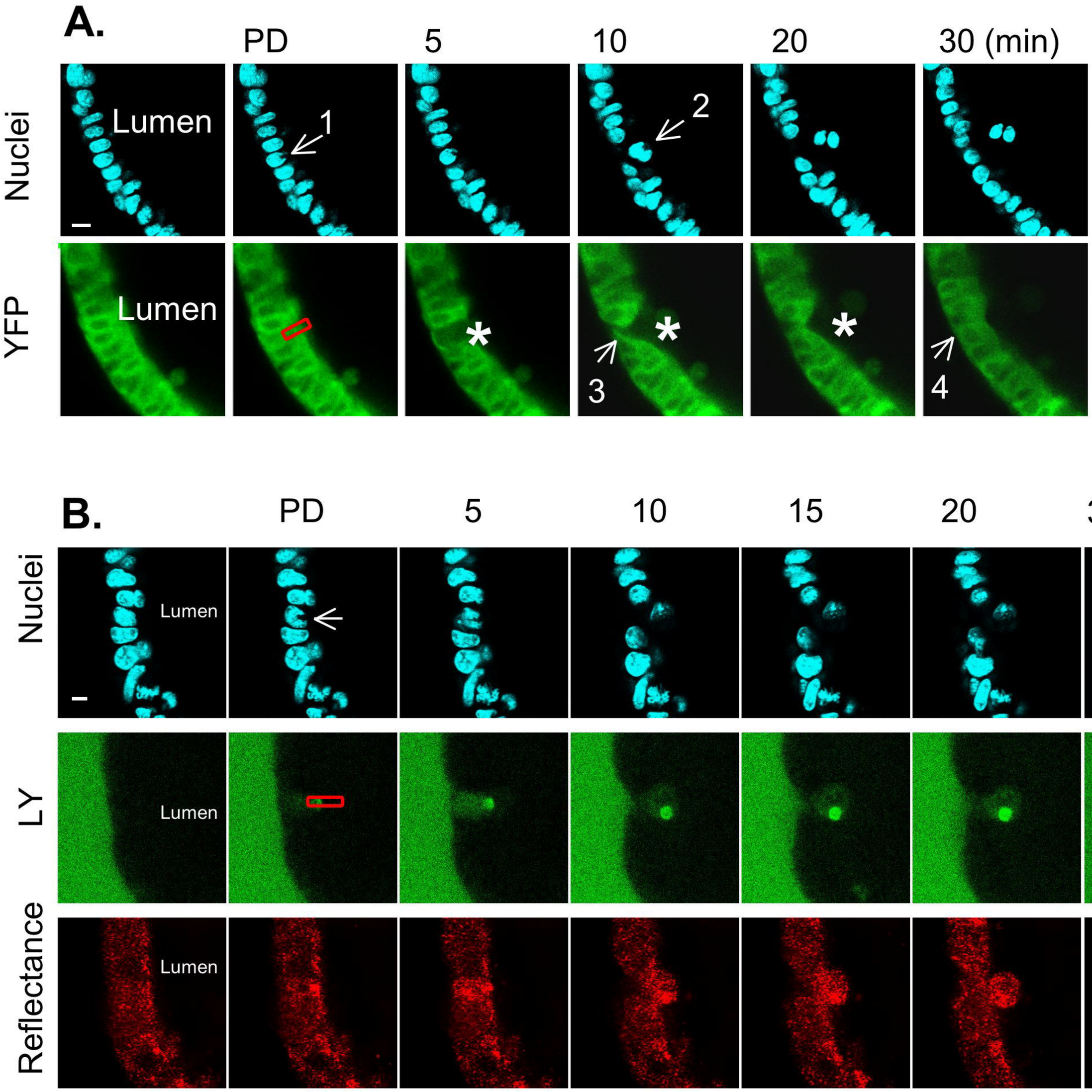
A.
PD
5
10
20
30 (min)
Nuclei
YFP
Lumen
1
2
3
4
B.
PD
5
10
15
20
30 (min)
Nuclei
LY
Reflectance
Lumen